THESIS FOR THE DEGREE OF LICENTIATE OF ENGINEERING

Conjugate Priors for Bayesian Object Tracking

Yuxuan Xia

Department of Electrical Engineering
Chalmers University of Technology
Gothenburg, Sweden, 2020

Conjugate Priors for Bayesian Object Tracking

Yuxuan Xia

ISSN 1403-266X
This thesis has been prepared using LaTeX.

Department of Electrical Engineering
Chalmers University of Technology
SE-412 96 Gothenburg, Sweden
Phone: +46 (0)31 772 1000
www.chalmers.se

Printed by Chalmers Reproservice
Gothenburg, Sweden, September 2020

To my family.

Abstract

Object tracking refers to the problem of using noisy sensor measurements to determine the location and characteristics of objects of interest in clutter. Nowadays, object tracking has found applications in numerous research venues as well as application areas, including air traffic control, maritime navigation, remote sensing, intelligent video surveillance, and more recently environmental perception, which is a key enabling technology in autonomous vehicles. This thesis studies conjugate priors for Bayesian object tracking with focus on multi-object tracking (MOT) based on sets of trajectories. Finite Set Statistics provides an elegant Bayesian formulation of MOT in terms of the theory of random finite sets (RFSs). Conjugate priors are also of great interest as they provide families of distributions that are suitable to work with when seeking accurate approximations to the true posterior distributions. Many RFS-based MOT approaches are only concerned with multi-object filtering without attempting to estimate object trajectories. An appealing approach to building tracks is by computing the multi-object densities on sets of trajectories. This leads to the development of trajectory filters, e.g., filters based on Poisson multi-Bernoulli mixture (PMBM) conjugate priors.

In this thesis, [Paper A] and [Paper B] consider the problem of point object tracking where an object generates at most one measurement per scan. In [Paper A], it is shown that the trajectory MBM filter is the solution to the MOT problem for standard point object models with multi-Bernoulli birth. In addition, the multi-scan implementations of trajectory PMBM and MBM filters are presented. In [Paper B], a solution for recovering full trajectory information, via the calculation of the posterior of the set of trajectories from a sequence of multi-object filtering densities and the multi-object dynamic model, is presented. [Paper C] and [Paper D] consider the problem of extended object tracking where an object may generate multiple measurements per scan. In [Paper C], the extended object PMBM filter for sets of objects is generalized to sets of trajectories. In [Paper D], a learning-based extended object tracking algorithm using a hierarchical truncated Gaussian measurement model tailored for automotive radar measurements is presented.

Keywords: Bayesian estimation, conjugate prior, object tracking, extended object, automotive radar, multi-object tracking, multi-object smoothing, backward simulation, random finite sets, sets of trajectories.

List of Publications

This thesis is based on the following publications:

[A] **Yuxuan Xia**, Karl Granström, Lennart Svensson,
Ángel F. García-Fernández, Jason L. Williams, "Multi-scan implementation of the trajectory Poisson multi-Bernoulli mixture filter". Published in Journal of Advances in Information Fusion, Dec. 2019.

[B] **Yuxuan Xia**, Lennart Svensson, Ángel F. García-Fernández,
Karl Granström, Jason L. Williams, "Backward simulation for sets of trajectories". Published in 23rd International Conference on Information Fusion, Jul. 2020.

[C] **Yuxuan Xia**, Karl Granström, Lennart Svensson,
Ángel F. García-Fernández, Jason L. Williams, "Extended target Poisson multi-Bernoulli mixture trackers based on sets of trajectories". Published in 22nd International Conference on Information Fusion, Jul. 2019.

[D] **Yuxuan Xia**, Pu Wang, Karl Berntorp, Lennart Svensson,
Karl Granström, Hassan Mansour, Petros Boufounos, Philip V. Orlik, "Learning based extended object tracking using hierarchical truncation measurement model with automotive radar". Submitted to IEEE Journal of Selected Topics in Signal Processing, 2020.

Other publications by the author, not included in this thesis, are:

[E] **Y. Xia**, P. Wang, K. Berntorp, P. Boufounos, P. Orlik, L. Svensson, K. Granström, "Extended object tracking with automotive radar using learned structural measurement model". *IEEE Radar Conference (RadarConf)*, Florence, Italy, Sep. 2020.

[F] **Y. Xia**, P. Wang, K. Berntorp, H. Mansour, P. Boufounos, P. Orlik, "Extended object tracking using hierarchical truncation model with partial-view measurements". *IEEE 11th Sensor Array and Multichannel Signal Processing Workshop (SAM)*, Hangzhou, China, Jun. 2020.

[G] **Y. Xia**, P. Wang, K. Berntorp, T. Koike-Akino, H. Mansour, M. Pajovic, P. Boufounos, P. Orlik, "Extended object tracking using hierarchical

truncation measurement model with automotive radar". *IEEE International Conference on Acoustics, Speech and Signal Processing (ICASSP)*, Barcelona, Spain, May. 2020.

[H] **Y. Xia**, K. Granström, L. Svensson, Ángel F. García-Fernández, "An implementation of the Poisson multi-Bernoulli mixture trajectory filter via dual decomposition". *21st International Conference on Information Fusion (FUSION)*, Cambridge, United Kingdom, Jul. 2018.

[I] **Y. Xia**, K. Granström, L. Svensson, Ángel F. García-Fernández, "Performance evaluation of multi-Bernoulli conjugate priors for multi-target filtering". *20th International Conference on Information Fusion (FUSION)*, Xi'an, China, Jul. 2017.

[J] Ángel F. García-Fernández, L. Svensson, Jason L. Williams, **Y. Xia**, K. Granström, "Trajectory Poisson multi-Bernoulli filters". *IEEE Transactions on Signal Processing*, vol. 68, pp. 4933–4945, Aug. 2020.

[K] Ángel F. García-Fernández, L. Svensson, Jason L. Williams, **Y. Xia**, K. Granström, "Trajectory multi-Bernoulli filters for multi-target tracking based on sets of trajectories". *23nd International Conference on Information Fusion (FUSION)*, Rustenburg, South Africa, Jul. 2020.

[L] K. Granström, L. Svensson, **Y. Xia**, Ángel F. García-Fernández, Jason L. Williams, "Spatiotemporal constraints for sets of trajectories with applications to PMBM densities". *23nd International Conference on Information Fusion (FUSION)*, Rustenburg, South Africa, Jul. 2020.

[M] Ángel F. García-Fernández, **Y. Xia**, K. Granström, L. Svensson, Jason L. Williams, "Gaussian implementation of the multi-Bernoulli mixture filter". *22rd International Conference on Information Fusion (FUSION)*, Ottawa, Canada, Jul. 2019.

[N] K. Granström, L. Svensson, **Y. Xia**, Ángel F. García-Fernández, Jason L. Williams, "Poisson multi-Bernoulli mixture trackers: continuity through random finite sets of trajectories". *21st International Conference on Information Fusion (FUSION)*, Cambridge, United Kingdom, Jul. 2018.

[O] K. Granström, L. Svensson, S. Reuter, **Y. Xia**, M. Fatemi, "Likelihood-based data association for extended object tracking using sampling methods". *IEEE Transactions on Intelligent Vehicles*, vol. 3, no. 1, pp. 30–45, Dec. 2017.

Acknowledgments

As my Ph.D. journey has been half-way through now, I would like to take this opportunity to express my appreciation to the people, without whom this thesis would not have been possible.

I would like to first thank my examiner and supervisor Prof. Lennart Svensson and my previous supervisor Dr. Karl Granström now at Embark Trucks for drawing up the research project and their immense help and support on my researches. Their enthusiasm, encouragement and patience stimulate me to be a better researcher.

I would like to thank Dr. Ángel F. García-Fernández at Liverpool university for the stimulating discussions as well as the timely and detailed feedback on the papers we have collaborated. I would also like to thank Dr. Jason L. Williams at CSIRO for his research ideas and insightful comments on the manuscripts. I am also grateful to Dr. Daniel Svensson at Zenseact for being the coordinator of my Ph.D. project and the discussions we have had during the project meetings.

I would like to thank Dr. Pu (Perry) Wang for being my host and for all the supports I received from you during my internship at MERL. I would also like to thank Dr. Karl Berntorp, Dr. Petros Boufounos, Dr. Philip Orlik, Dr. Hassan Mansou and other researchers in MERL's signal processing group for all the interesting academic discussions.

I would like to thank Assoc. Prof. Lars Hammarstrand. It has been a nice experience being a teaching assistant of the Sensor Fusion and Nonlinear Filtering course that you teach. I would also like to thank the deputy head of the department, also the head of the signal processing group, Prof. Tomas McKelvey as well as all the current and former colleagues in the signal processing group for jointly maintaining a pleasant research atmosphere. Many thanks also to my Chinese "gang" in the department for all the joyful time we have had together.

Last but not the least, my deepest thanks go to my family for their love, understanding and support all the way in my journey towards a Ph.D. degree.

Yuxuan Xia
Göteborg, October, 2020

Acronyms

CPHD:	Cardinalized probability hypothesis density
EKF:	Extended Kalman filter
EOT:	Extended object tracking
GGIW:	Gamma Gaussian inverse-Wishart
GLMB:	Generalized labeled multi-Bernoulli
GNN:	Global nearest neighbor
GOSPA:	Generalized optimal sub-pattern assignment
GWD:	Gaussian Wasserstein distance
HTG:	Hierarchical truncated Gaussian
JMPD:	Joint multitarget probability density
JPDA:	Joint probabilistic data association
KLD:	Kullback-Leibler divergence
LMB:	Labeled multi-Bernoulli
MB:	Multi-Bernoulli
MBM:	Multi-Bernoulli mixture
MHT:	Multiple hypothesis tracker
MOT:	Multi-object tracking
OSPA:	Optimal sub-pattern assignment
PGFL:	Probability generating functionals
PHD:	Probability hypothesis density
PMB:	Poisson multi-Bernoulli

PMBM:	Poisson multi-Bernoulli mixture
PPP:	Poisson point process
RFS:	Random finite set
RTSS:	Rauch-Tung-Striebel smoother

Contents

Part I

Overview

CHAPTER 1

Introduction

1.1 Background

Object/target tracking refers to the problem of using sensor measurements to determine the location, trajectory and characteristics of objects of interest [1], [2]. Initially driven by aerospace and defense applications, object tracking has a long history spanning over decades. In recent times, with the advances in object tracking techniques as well as sensing and computing technologies, there has been an explosion in the use of object tracking technology in numerous research venues as well as application areas, including air traffic control, maritime navigation, remote sensing, biomedical research, intelligent video surveillance, and more recently environmental perception, which is a key enabling technology in autonomous vehicles.

This thesis studies Bayesian object tracking algorithms. Bayes's theorem provides an elegant and powerful probabilistic framework to solve the object tracking problem. The goal of Bayesian estimation in object tracking is to compute the posterior density of the random variables of interest, which encapsulates all the information contained in the measurements [3]. In object tracking, the object may not always be detected and the sensor measurements

are noisy and contain clutter. If detected, the object may occupy multiple sensor resolution cells, depending on its distance to the sensor and the sensor resolution. Conventional tracking algorithms consider the problem of point object tracking with the assumption that an object gives rise to at most one measurement per scan. The tracking of an object that gives rise to a varying number of measurements per scan is called extended object tracking (EOT) [4], which has found more applications with the development of high-resolution sensors such as automotive radar and lidar [5]–[8].

Automotive radar plays an important role in autonomous driving as it provides reliable environmental perception in all-weather conditions with affordable cost [9]. For an extended object, it is often assumed that the measurements are spatially distributed as a function of individual measurement likelihoods, also referred to as the spatial distribution. To capture the spatial characteristics of real-world automotive radar measurements, the development of spatial models tailored to automotive radar measurements have started to attract more attention in recent years. Moreover, with the release of large-scale automotive radar datasets, data-driven approaches are becoming a hot spot of EOT with automotive radar.

In a multi-object scenario, the measurements may originate from one of the various objects and the number of objects is time-varying due to objects appearing in and disappearing from the surveillance area [10]. Fundamental to this problem is the estimation of both the number of objects and their trajectories by partitioning measurements into the sets of measurements originating from different objects and false alarms. The major approaches to multi-object tracking (MOT) include the global nearest neighbor (GNN) filter, the joint probabilistic data association (JPDA) filter [11], the multiple hypothesis tracker (MHT) [12], and random finite sets (RFSs) based multi-object filters. Finite Set Statistics [13] provides a theoretically elegant Bayesian formulation of MOT in terms of the theory of RFSs where the multi-object state is represented as a finite set of single-object states [14], [15].

Exact closed-form solutions of RFS-based MOT Bayes filters are given by multi-object conjugate priors [16], which are defined as "if we start with the proposed conjugate initial prior, then all subsequent predicted and posterior distributions have the same form as the initial prior". MOT conjugate priors are of great interest as they provide families of distributions that are suitable to work with when seeking accurate approximations to the true posterior

distributions.

Two well-established MOT conjugate priors are the Poisson multi-Bernoulli mixture (PMBM) [17], based on unlabeled RFSs, and the generalized labeled multi-Bernoulli (GLMB) [16], based on labeled RFSs. The difference between these two MOT conjugate priors mainly lies in the modeling of newborn objects, i.e., objects appearing in the surveillance area. With Poisson point process (PPP) birth model, the solution to the multi-object filtering problem is given by the PMBM filter [18], [19]. If the birth model is multi-Bernoulli (MB) instead of Poisson, the filtering density is given by the multi-Bernoulli mixture (MBM) filter, which corresponds to the PMBM filtering recursion by setting the intensity of the Poisson process to zero and adding Bernoulli components for newborn objects in the prediction step [20]. The MBM filter can also be extended to consider MBs with deterministic object existence, which we refer to as the MBM_{01} filter, at the expense of increasing the number of global hypotheses [18]. Both MBM and MBM_{01} filters can consider object states with labels, and the (labeled) MBM_{01} filtering recursion is analogous to the δ-GLMB filtering recursion [21], [22].

Vector-type MOT methods, e.g., the JPDA filter and the MHT, describe the multi-object states and measurements by random vectors. They explicitly estimate trajectories; i.e., they associate a state estimate with a previous state estimate or declare the appearance of a new object. For MOT methods based on set representations, time sequences of tracks cannot be constructed easily as the multi-object states are order independent. For this reason, many RFS-based MOT approaches, e.g., the probability hypothesis density (PHD) filter [23] and the cardinalized PHD (CPHD) filter [24], are only concerned with multi-object filtering, in which one aims to estimate the current set of objects, without attempting to estimate object trajectories. The PMBM filter has a hypothesis structure similar to MHT [25], however, track continuity in the form of trajectories is not explicitly established as the posterior itself only provides information about the current set of objects. A categorization of the multi-object filters mentioned so far is illustrated in Fig. 1.1.

One approach to building trajectories from posterior densities is to add unique labels to the object states and form trajectories by linking object state estimates with the same label [16], [26], [27]. Sequential track building approaches based on labeling can work well in many cases but it is not always adequate due to ambiguity in object-to-label associations, e.g., when object

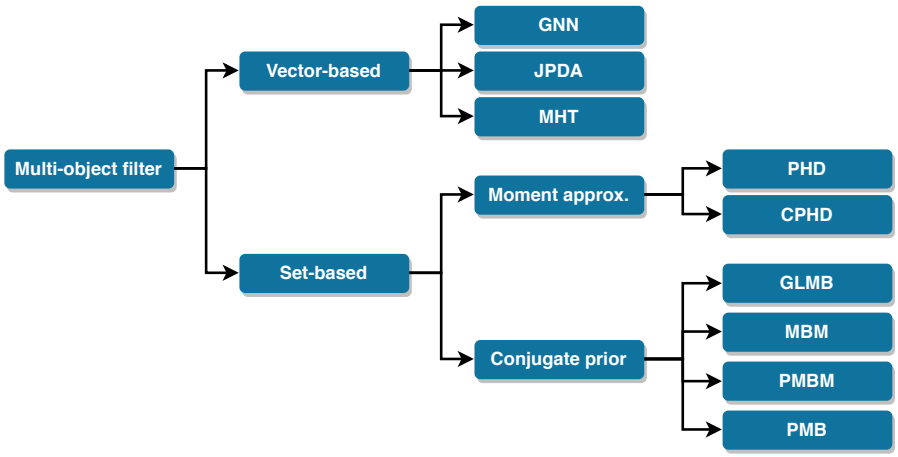

Figure 1.1: A chart categorizing different multi-object filters.

birth is independent and identically distributed, and when objects get in close proximity and then separate. The above track building problems can be solved by computing multi-object densities on sets of trajectories [28]. This leads to the development of trajectory filters including, for example, the trajectory PHD filter [29], the trajectory CPHD filter [29], the trajectory PMBM filter [30] and its approximation the trajectory PMB filter [31].

Bayes filters use the measurements obtained before and at the current time step for computing the estimate of the current object state. However, sometimes it is also interesting to exploit the entire measurement history to arrive at more accurate object state estimates at all of the preceding time steps. This problem can be solved with Bayesian smoothing. The multi-object generalization of a Bayes smoother is an algorithm that computes the multi-object densities at all of the preceding time steps given the entire batch of measurements. Existing literature on multi-object smoothing [15, Chapter 14] only focus on computing the multi-object smoothing densities at each time step, which, even if labeled, may not be enough to provide trajectory information. Multi-object trajectory filters compute the filtering densities of sets of trajectories and therefore are able to directly produce smoothed trajectory estimates using e.g., the accumulated state densities [32]. Nevertheless, there are many MOT methods in the literature that can efficiently estimate the object states

but that cannot easily produce trajectory estimation in a principled manner. Therefore, how to leverage on filters that do not keep trajectory information to compute the posterior density of sets of trajectories needs further investigation.

Contributions

This thesis investigates Bayesian object tracking methods for both point object and extended object, with particular focus on Bayesian MOT methods based on sets of trajectories. [Paper A] and [Paper B] consider the problem of point object tracking. In [Paper A], the filtering recursions for the trajectory MBM filter and the trajectory MBM_{01} filter using an MB birth model are presented. In addition, the multi-scan implementations of trajectory PMBM, MBM and MBM_{01} filters using dual decomposition and N-scan pruning are proposed. In [Paper B], a solution for multi-object smoothing is presented. The proposed multi-object smoother computes the posterior of the set of trajectories from a sequence of multi-object filtering densities and the multi-object dynamic model.

[Paper C] and [Paper D] consider the problem of extended object tracking. In [Paper C], the extended object PMBM filter for sets of objects is extended to sets of trajectories. Specifically, the prediction and update equations of two trajectory PMBM filters for extended object tracking are presented: one in which the set of current (i.e., "alive") trajectories is tracked, and one in which the set of all trajectories (both "dead" and "alive") up to the current time is tracked. In [Paper D], a data-driven measurement model EOT with automotive radar is presented, in which the spatial distribution of automotive radar measurements is modeled as a hierarchical truncated Gaussian (HTG) with structural geometry parameters that can be learned from the training data. The learned HTG measurement model is further incorporated into a random matrix based EOT approach with two (multi-sensor) measurement updates.

1.2 Thesis outline

The remainder of Part I of the thesis is organized as follows. Chapter 2 reviews Bayesian filtering and smoothing in dynamical systems. Chapter 3 covers

the basic concepts and properties of random finite sets as well as metrics for tracking performance evaluation. Chapter 4 introduces the multi-object dynamic and measurement models used in this thesis. Chapter 5 presents the single-object and multi-object conjugacy for object tracking. Chapter 6 is about multi-object tracking based on sets of trajectories. Chapter 7 provides a summary of the included papers in this thesis. Chapter 8 summarizes the conclusions and possible future work directions. Part II of the thesis includes the appended papers.

1.3 Notation

This section introduces the notations used in Part I of the thesis. Vectors are generally represented by lower-case letters (e.g., x). Matrices are generally represented by upper-case letters (e.g. X). Sets of vectors are represented by bold lower-case letters (e.g., $\mathbf{x}$). Sets of trajectories are represented by bold upper-case letters (e.g., $\mathbf{X}$). Classes of distributions are represented by calligraphy letters (e.g, $\mathcal{X}$). Spaces are generally represented by blackboard bold letters. For example, the n-dimensional Euclidean space is denoted by $\mathbb{R}^n$ and the space of positive integers is denoted by $\mathbb{N}$. The more general spaces are represented by fraktur letters (e.g., $\mathfrak{X}$). The class of finite subsets of a space $\mathfrak{X}$ is represented by $\mathcal{F}(\mathfrak{X})$.

CHAPTER 2

Bayesian filtering and smoothing

Bayesian filtering and smoothing refer to a class of methods that can be used for estimating the state of a dynamical system which is indirectly observed through noisy measurements. This chapter covers the basic aspects of Bayesian filtering and smoothing. The reader is referred to [3] for further readings on this topic.

2.1 Bayesian inference in dynamical systems

The state of the dynamical system at time step k is denoted as $x_k \in \mathbb{R}^{n_x}$ where n_x is the dimension of the state. In the context of object tracking, x_k may represent the object's position, velocity and any other motion parameters of interest of the object at time step k. The state has an initial prior density $p(x_0)$ at time 0, and it evolves in time according to a Markov system with transition density $p(x_k|x_{k-1})$. At each time step k, the state is observed through a noisy measurement $z_k \in \mathbb{R}^{n_z}$ whose density is $p(z_k|x_k)$. Let $x_{0:k} = (x_0, x_1, \ldots, x_k)$ denote the sequence of states from time step 0 to k. Note that in object tracking the sequence $x_{0:k}$ is used to represent the object trajectory up to time step k. Also, let $z_{1:k} = (z_1, \ldots, z_k)$ denote the sequence of states from

time step 1 to k. The joint density of all the states and measurements up to time step k is given by

$$p(x_{0:k}, z_{1:k}) = p(x_0) \prod_{j=1}^{k} p(x_j|x_{j-1}) p(z_j|x_j). \tag{2.1}$$

In the Bayesian framework, all information of interest about the state sequence $x_{0:k}$ is given by the posterior density $p(x_{0:k}|z_{1:k})$, which denotes the density of $x_{0:k}$ given the measurement sequence $z_{1:k}$. This density can be computed by applying Bayes' rule on (2.1)

$$\begin{aligned} p(x_{0:k}|z_{1:k}) &= \frac{p(x_{0:k}, z_{1:k})}{p(z_{1:k})} \\ &= \frac{p(x_0) \prod_{j=1}^{k} p(x_j|x_{j-1}) p(z_j|x_j)}{p(z_{1:k})} \end{aligned} \tag{2.2}$$

where $p(z_{1:k})$ is the normalization constant defined as

$$p(z_{1:k}) = \int p(x_{0:k}, z_{1:k}) dx_{0:k}. \tag{2.3}$$

Because it is intractable to compute the posterior density (2.2) on the state sequence without approximations for long time sequences, Bayesian inference in dynamical systems usually focuses on the following simpler problems:

- Filtering: the objective is to compute the density $p(x_k|z_{1:k})$ of the current state x_k given the measurements up to the current time step.
- Smoothing: the objective is to compute the density $p(x_j|z_{1:k})$ of a past state x_j with $0 \leq j < k$ given the measurements up to the current time step k.
- Prediction: the objective is to compute the density $p(x_j|z_{1:k})$ of a future state x_j with $j > k$ given the measurements up to the current time step k.

However, sometimes it is actually necessary to approximate the posterior density on the state sequence rather than focusing on simpler problems, such as filtering or smoothing. Typical examples include backward simulation particle smoother [33], view-based simultaneous localization and mapping using

delayed-state filters [34] and MOT where the objective is to infer object trajectories [28].

2.2 Bayesian filtering

In Bayesian filtering, the objective is to compute the filtering density $p(x_k|z_{1:k})$. This can be done using Bayesian filtering recursion, which consists of two steps, prediction and update. Given the filtering density $p(x_{k-1}|z_{1:k-1})$ and the transition density $p(x_k|x_{k-1})$ at time step $k-1$, the predicted density $p(x_k|z_{1:k-1})$ is given by the Chapman-Kolmogorov equation

$$p(x_k|z_{1:k-1}) = \int p(x_k|x_{k-1})p(x_{k-1}|z_{1:k-1})dx_{k-1}. \tag{2.4}$$

In the update step, given the predicted density $p(x_k|z_{1:k-1})$ and the measurement distribution $p(z_k|x_k)$ at time step k, the filtering density at time k is given by Bayes' rule

$$p(x_k|z_{1:k-1}) = \frac{p(z_k|x_k)p(x_k|z_{1:k-1})}{p(z_k|z_{1:k-1})} \tag{2.5}$$

where the normalization constant is

$$p(z_k|z_{1:k-1}) = \int p(z_k|x_k)p(x_k|z_{1:k-1})dx_k. \tag{2.6}$$

Kalman filtering

The Kalman filter is the closed-form solution to the Bayesian filtering equations for linear Gaussian dynamic and measurement models:

$$p(x_k|x_{k-1}) = \mathcal{N}(x_k; F_{k-1}x_{k-1}, Q_{k-1}), \tag{2.7a}$$
$$p(z_k|x_k) = \mathcal{N}(z_k; H_k x_k, R_k) \tag{2.7b}$$

where $F_{k-1} \in \mathbb{R}^{n_x,n_x}$ is the transition matrix, $Q_{k-1} \in \mathbb{R}^{n_x,n_x}$ is the covariance matrix of the process noise, $H_k \in \mathbb{R}^{n_z,n_x}$ is the observation matrix and $R_k \in \mathbb{R}^{n_z,n_z}$ is the covariance matrix of the measurement noise. The prior density of the state at time 0 is $p(x_0) = \mathcal{N}(x_0; \bar{x}_{0|0}, P_{0|0})$, where $\bar{x}_{0|0}$ and $P_{0|0}$ are the mean and covariance matrix of the state at time step 0.

The prediction and filtering densities at time step k are Gaussian and denoted as

$$p(x_k|z_{1:k-1}) = \mathcal{N}(x_k; \bar{x}_{k|k-1}, P_{k|k-1}), \tag{2.8a}$$
$$p(x_k|z_{1:k}) = \mathcal{N}(x_k; \bar{x}_{k|k}, P_{k|k}) \tag{2.8b}$$

where $\bar{x}_{k|k-1}$ and $P_{k|k-1}$ are the mean and the covariance of the predicted density and $\bar{x}_{k|k}$ and $P_{k|k}$ are the mean and the covariance of the filtering density. The parameters of the distributions (2.8) can be computed with the following Kalman filter prediction and update steps.

- The prediction step is

$$\bar{x}_{k|k-1} = F_{k-1}\bar{x}_{k-1|k-1}, \tag{2.9a}$$
$$P_{k|k-1} = F_{k-1}P_{k-1|k-1}F_{k-1}^{\mathrm{T}} + Q_{k-1}. \tag{2.9b}$$

- The update step is

$$\bar{x}_{k|k} = \bar{x}_{k|k-1} + \Psi_k S_k^{-1}(z_k - \bar{z}_k), \tag{2.10a}$$
$$P_{k|k} = P_{k|k-1} - \Psi_k S_k^{-1}\Psi_k^{\mathrm{T}}, \tag{2.10b}$$
$$\bar{z}_k = H_k\bar{x}_{k|k-1}, \tag{2.10c}$$
$$\Psi_k = P_{k|k-1}H_k^{\mathrm{T}}, \tag{2.10d}$$
$$S_k = H_k P_{k|k-1}H_k^{\mathrm{T}} + R_k \tag{2.10e}$$

where Ψ_k and S_k are usually referred to as the Kalman gain and the innovation covariance, respectively. The recursion is started from the prior mean $\bar{x}_{0|0}$ and covariance $P_{0|0}$.

Extended Kalman filter

The Kalman filter is not appropriate when the dynamic and measurement models are not linear. However, the filtering distributions of nonlinear models can often be approximated by Gaussian distributions. The extended Kalman filter (EKF) is a nonlinear Kalman filter based on Taylor series expansions. For dynamical systems with additive Gaussian noise, the transition and mea-

surement densities have the form [3, Chapter 5]

$$p(x_k|x_{k-1}) = \mathcal{N}(x_k; f_{k-1}(x_{k-1}), Q_{k-1}), \tag{2.11a}$$
$$p(z_k|x_k) = \mathcal{N}(z_k; h_k(x_k), R_k) \tag{2.11b}$$

where $f_{k-1}(\cdot)$ and $h_k(\cdot)$ are possibly nonlinear dynamic and measurement model functions, respectively.

The idea of the EKF is to assume Gaussian approximations

$$p(x_k|z_{1:k-1}) \approx \mathcal{N}(x_k; \bar{x}_{k|k-1}, P_{k|k-1}), \tag{2.12a}$$
$$p(x_k|z_{1:k}) \approx \mathcal{N}(x_k; \bar{x}_{k|k}, P_{k|k}) \tag{2.12b}$$

to the prediction and filtering densities using first-order Taylor series approximations to the non-linearities $f_{k-1}(\cdot)$ and $h_k(\cdot)$ around $\bar{x}_{k-1|k-1}$ and $\bar{x}_{k|k-1}$, respectively. Let $F_{k-1}(\bar{x}_{k-1|k-1})$ be the Jacobian matrix of $f_{k-1}(\cdot)$ evaluated at $\bar{x}_{k-1|k-1}$ and let $H_k(\bar{x}_{k|k-1})$ be the Jacobian matrix of $h_k(\cdot)$ evaluated at $\bar{x}_{k|k-1}$. The parameters of the distributions (2.11) can then be computed with the following EKF prediction and update steps.

- The prediction step is

$$\bar{x}_{k|k-1} = f_{k-1}(\bar{x}_{k-1|k-1}), \tag{2.13a}$$
$$P_{k|k-1} = F_{k-1}(\bar{x}_{k-1|k-1})P_{k-1|k-1}F_{k-1}(\bar{x}_{k-1|k-1})^{\mathrm{T}} + Q_{k-1}. \tag{2.13b}$$

- The update step is

$$\bar{x}_{k|k} = \bar{x}_{k|k-1} + \Psi_k S_k^{-1}(z_k - \bar{z}_k), \tag{2.14a}$$
$$P_{k|k} = P_{k|k-1} - \Psi_k S_k^{-1}\Psi_k^{\mathrm{T}}, \tag{2.14b}$$
$$\bar{z}_k = h_k(\bar{x}_{k|k-1}), \tag{2.14c}$$
$$\Psi_k = P_{k|k-1}H_k(\bar{x}_{k|k-1})^{\mathrm{T}}, \tag{2.14d}$$
$$S_k = H_k(\bar{x}_{k|k-1})P_{k|k-1}H_k(\bar{x}_{k|k-1})^{\mathrm{T}} + R_k. \tag{2.14e}$$

Other non-linear Kalman filter based on Gaussian approximations including, for example, the posterior linearized filter (PLF) [35], unscented Kalman filter [36], cubature Kalman filter [37], and iterated approaches, such as iterative EKF and iterative PLF [35].

2.3 Bayesian smoothing

In Bayesian smoothing, the objective is to compute the smoothing density $p(x_k|z_{1:K})$, which is the distribution of the state x_k at time step k after receiving the measurements up to a time step K where $K > k$. The backward recursive equation for computing the smoothed densities $p(x_k|z_{1:K})$ for any $k < K$ is given by

$$p(x_k|z_{1:K}) = p(x_k|z_{1:k}) \int \frac{p(x_{k+1}|x_k)p(x_{k+1}|z_{1:K})}{p(x_{k+1}|z_{1:K})} dx_{k+1} \tag{2.15}$$

where $p(x_k|z_{1:k})$ is the filtering density at time step k and $p(x_{k+1}|z_{1:k})$ is the predicted density at time step $k+1$.

Rauch-Tung-Striebel smoother

The Rauch-Tung-Striebel smoother (RTSS) [38] gives the closed-form smoothing solution to linear Gaussian models. The smoothing density at time step k is Gaussian and denoted as

$$p(x_k|z_{1:K}) = \mathcal{N}(x_k; \bar{x}_{k|K}, P_{k|K}) \tag{2.16}$$

where $\bar{x}_{k|K}$ and $P_{k|K}$ are the mean and the covariance of the smoothed density, respectively. The parameters of the distribution (2.16) can be computed with the following backward recursion equations [38]:

$$G_k = P_{k|k} F_k^{\mathrm{T}} P_{k+1|k}^{-1}, \tag{2.17a}$$

$$\bar{x}_{k|K} = \bar{x}_{k|k} + G_k(\bar{x}_{k+1|K} - \bar{x}_{k+1|k}), \tag{2.17b}$$

$$P_{k|K} = P_{k|k} + G_k(P_{k+1|K} - P_{k+1|k})G_k^{\mathrm{T}} \tag{2.17c}$$

where $\bar{x}_{k|k}$ and $P_{k|k}$ are the mean and covariance computed by the Kalman update and $\bar{x}_{k+1|k}$ and $P_{k+1|k}$ are the mean and covariance computed by the Kalman prediction. The recursion is started from the last time step K with $\bar{x}_{K|K}$ and $P_{K|K}$.

Backward simulation

Bayesian inference in dynamical systems often requires generating samples from the posterior density $p(x_{0:K}|z_{1:K})$. This problem can be addressed using backward simulation [33]. An alternative recursion for the posterior density $p(x_{k:K}|z_{1:K})$ without marginalizing out the states after time step k is

$$\begin{aligned} p(x_{k:K}|z_{1:K}) &= p(x_k|x_{k+1}, z_{1:K})p(x_{k+1:K}|z_{1:K}), \\ &= p(x_k|x_{k+1}, z_{1:k})p(x_{k+1:K}|z_{1:K}), \end{aligned} \tag{2.18}$$

where $p(x_k|x_{k+1}, z_{1:k})$ is usually referred to as the backward kernel. The recursion (2.18) evolves backward in time and starts with the filtering density $p(x_K|z_{1:K})$ at time step K.

Using (2.18), the posterior density $p(x_{0:K}|z_{1:K})$ can be factorized as

$$p(x_{0:K}|z_{1:K}) = p(x_0) \left(\prod_{j=1}^{K-1} p(x_j|x_{j+1}, z_{1:j}) \right) p(x_K|z_{1:K}). \tag{2.19}$$

Initially, a sample is generated from the filtering density $p(x_K|z_{1:K})$ at time step K,

$$x_K \sim p(x_K|z_{1:K}). \tag{2.20}$$

Then this backward trajectory is successively augmented with samples generated from $p(x_k|x_{k+1}, z_{1:k})$,

$$x_k \sim p(x_k|x_{k+1}, z_{1:k}), \tag{2.21}$$

for $k = K-1, \ldots, 1$. At time step 0, the backward trajectory is augmented with a sample generated from the initial prior density $p(x_0)$. After a complete backward sweep, the backward trajectory $x_{0:k}$ can be regarded as a realization from the posterior density $p(x_{0:K}|z_{1:K})$.

For linear Gaussian models, the backward kernel density $p(x_k|x_{k+1}, z_{1:k})$ is a Gaussian

$$p(x_k|x_{k+1}, z_{1:k}) = \mathcal{N}(x_k; \mu_k, M_k), \tag{2.22}$$

with

$$\mu_k = \bar{x}_{k|k} + G_k(x_{k+1} - F_k\bar{x}_{k|k}), \tag{2.23a}$$
$$M_k = P_{k|k} - G_k F_k P_{k|k} \tag{2.23b}$$

where G_k is the smoothing gain (2.17a) in RTSS, and $\bar{x}_{k|k}$ and $P_{k|k}$ are the mean and covariance of the filtering density $p(x_k|z_{1:k})$ computed by a Kalman filter.

CHAPTER 3

Random finite sets and metrics

Random finite sets (RFSs) are set-valued random variables whose elements and cardinality are random. This chapter covers the basic concepts and relevant properties of RFSs that will be used in the rest of the thesis. The reader is referred to [14], [15] for further readings on this topic. Common metrics used for tracking performance evaluation are also introduced.

3.1 Definition

Let $\mathfrak{Y}$ be an underlying space, such as a single-object state space $\mathfrak{X}$. The state of a single-object contains the information of interest about the object, which is usually represented by an n-dimensional vector x in some Euclidean space $\mathbb{R}^n$. An RFS is a random variable $\mathbf{x}$ on the set $\mathcal{F}(\mathfrak{X})$ of all the finite subsets of $\mathfrak{X}$. In general, $\mathfrak{Y}$ can be any Hausdorff, locally compact, and completely separable topological space [15, Appendix B]. In this thesis, the following three types of spaces that meet these properties are considered:

- The single-object state space $\mathfrak{X}$, which usually contains the object's location and any other motion parameters of interest.

- The single-measurement space $\mathbb{R}^{n_z}$ for measurement models based on detections, where n_z is the dimension of the single-measurement vector.
- The single-object trajectory space $\mathfrak{T}$, which contains the information that characterizes the trajectory of an object.

3.2 Multi-object statistics

This section covers basic multi-object concepts and statistics in terms of the the theory of RFSs.

Set integral and multi-object densities

Given a real-valued function $f(\cdot)$ on the space $\mathcal{F}(\mathbb{R}^{n_x})$, its set integral is defined as

$$\int f(\mathbf{x})\delta\mathbf{x} = \sum_{i=0}^{\infty} \frac{1}{i!} \int f(\{x_1, \ldots, x_i\}) dx_1 \cdots dx_i. \tag{3.1}$$

The set integral sums over all possible cardinalities and all possible object states for each cardinality. A function $f(\cdot)$ is a multi-object density, if $f(\cdot) \geq 0$ and its set integral is one.

Convolution formula for multi-object densities

Let $\mathbf{x}_1, \ldots, \mathbf{x}_n \subseteq \mathcal{F}(\mathfrak{X})$ be n statistically independent RFSs with multi-object densities $f_1(\cdot), \ldots, f_n(\cdot)$, respectively. Then the multi-object density $f(\cdot)$ of the union $\mathbf{y} = \mathbf{x}_1 \cup \cdots \cup \mathbf{x}_n$ is given by the convolution formula

$$f(\mathbf{y}) = \sum_{\mathbf{y}=\mathbf{x}_1 \uplus \cdots \uplus \mathbf{x}_n} \prod_{i=1}^{n} f_i(\mathbf{x}_i) \tag{3.2}$$

where $\uplus$ stands for disjoint union and the summation is taken over all mutually disjoint (and possibly empty) subsets $\mathbf{x}_1, \ldots, \mathbf{x}_n$ whose union is $\mathbf{y}$.

Probability generating functionals

Let h be a test function on the single-object space such that $h(x)$ is unitless and $0 \leq h(x) \leq 1$. The probability generating functionals (PGFL) of an RFS

$\mathbf{x}$ is defined as

$$G[h] = \int h^{\mathbf{x}} f(\mathbf{x}) \delta\mathbf{x} \tag{3.3}$$

where $f(\cdot)$ is the multi-object density of $\mathbf{x}$ and $h^{\mathbf{x}}$ is the power functional defined as

$$h^{\mathbf{x}} = \begin{cases} 1 & \text{if} \quad \mathbf{x} = \varnothing \\ \prod_{x \in \mathbf{x}} h(x) & \text{if} \quad \mathbf{x} \neq \varnothing. \end{cases} \tag{3.4}$$

The PGFL of an RFS completely characterizes its multi-object density, and it is useful for deriving multi-object filters.

Cardinality distribution

The cardinality of a set $\mathbf{x}$, denoted by $|\mathbf{x}|$, is the number of elements in the set. The number of elements of an RFS is a random variable and characterized by a probability mass function, which is referred to as the cardinality distribution. The cardinality distribution of an RFS with multi-object density $f(\cdot)$ is given by

$$\rho(n) = \frac{1}{n!} \int f(\{x_1, \ldots, x_n\}) dx_1 \cdots dx_n. \tag{3.5}$$

The number $\rho(n)$ is the probability that $\mathbf{x}$ contains n elements.

Probability hypothesis density

The probability hypothesis density (PHD), also referred to as the intensity function, of an RFS with multi-object density $f(\cdot)$ is defined on the single-object space $\mathfrak{X}$ as

$$\begin{aligned} D(x) &= \int f(\{x\} \cup \mathbf{x}) \delta\mathbf{x} \\ &= \sum_{i=0}^{\infty} \frac{1}{i!} \int f(\{x, x_1, \ldots, x_i\}) dx_1 \cdots dx_i. \end{aligned} \tag{3.6}$$

The integral of the PHD in a region $\mathbb{A} \subseteq \mathfrak{X}$ yields the expected number $\hat{N}_{\mathbb{A}}$ of objects in this region

$$\hat{N}_{\mathbb{A}} = \int_{\mathbb{A}} D(x) dx. \tag{3.7}$$

3.3 Multi-object processes

This section introduces some standard types of multi-object processes that will be used in this thesis. They are the Poisson RFSs, the Bernoulli RFSs, the multi-Bernoulli (MB) RFSs and the MB mixture (MBM) RFSs.

Poisson RFSs

In a Poisson RFS, also referred to as Poisson point process (PPP), the cardinality of the set is Poisson distributed and, for each cardinality, its elements are independent and identically distributed. The multi-object density for a Poisson RFS $\mathbf{x}$ is given by

$$f(\mathbf{x} = \{x_1, \ldots, x_n\}) = e^{-\lambda}\lambda^n \prod_{i=1}^{n} p(x_i) \tag{3.8}$$

where $\lambda \geq 0$ is the parameter of the Poisson cardinality distribution and $p(\cdot)$ denotes a single-object density. A Poisson RFS can be characterized by either its PHD/intensity function $D(x) = \lambda p(x)$ or by λ and $p(\cdot)$. Therefore the multi-object density of the Poisson RFS $\mathbf{x}$ can be alternatively expressed as

$$f(\mathbf{x} = \{x_1, \ldots, x_n\}) = e^{-\int D(x)dx} \prod_{i=1}^{n} D(x_i). \tag{3.9}$$

Bernoulli RFSs

In a Bernoulli RFS, the cardinality of the set is Bernoulli distributed. The multi-object density for a Bernoulli RFS $\mathbf{x}$ is given by

$$f(\mathbf{x}) = \begin{cases} 1 - r & \text{if} \quad \mathbf{x} = \varnothing \\ rp(x) & \text{if} \quad \mathbf{x} = x \end{cases} \tag{3.10}$$

where r is the probability of existence and $p(\cdot)$ is the single-object density of the object if it exists. A Bernoulli RFS is characterized by r and $p(\cdot)$.

Multi-Bernoulli RFSs

An MB RFS corresponds to the union of a finite number n of independent Bernoulli RFSs. The multi-object density of an MB RFS $\mathbf{x}$ is given by

$$f(\mathbf{x}) = \sum_{\mathbf{x}_1 \uplus \cdots \uplus \mathbf{x}_n = \mathbf{x}} \prod_{i=1}^{n} f_i(\mathbf{x}_i) \tag{3.11}$$

where $f_i(\cdot)$ is the ith Bernoulli component characterized by a probability r_i of existence and a single object density $p_i(\cdot)$. Therefore an MB RFS is characterized by the set $\{(r_1, p_1(\cdot)), \ldots, (r_n, p_n(\cdot))\}$.

Multi-Bernoulli mixture RFSs

An MB mixture (MBM) RFS is a weighted sum of MB RFSs. The multi-object density for an MBM RFS $\mathbf{x}$ is given by

$$f(\mathbf{x}) = \sum_{h=1}^{\mathcal{H}} w^h \sum_{\mathbf{x}_1 \uplus \cdots \uplus \mathbf{x}_n = \mathbf{x}} \prod_{i=1}^{n} f_i^h(\mathbf{x}_i) \tag{3.12}$$

where $w^1, \ldots, w^{\mathcal{H}}$ are non-negative weights such that $\sum_{i=1}^{\mathcal{H}} w^h = 1$ and $f_i^h(\mathbf{x}_i)$ are Bernoulli RFS densities for $i = 1, \ldots, n$ and $h = 1, \ldots, \mathcal{H}$.

A Bernoulli RFS density can be written as a mixture of Bernoulli RFS densities with probabilities of existence that are either zero or one. Therefore an MB can be expanded into an MBM_{01} with deterministic probabilities of existence in each Bernoulli component.

3.4 Metrics

This section introduces some standard single object metrics and MOT metrics for sets of objects.

Definition

It is important that the tracking performance is measured in a consistent way. Metrics ensure that the "distance" between the estimate and the truth

is mathematically meaningful. A metric d on a space $\mathfrak{X}$ is a distance function

$$d : \mathfrak{X} \times \mathfrak{X} \to [0, \infty) \tag{3.13}$$

where for all $x, y, z \in \mathfrak{X}$ the following four conditions are satisfied:

$$\text{Non-negativity:} \quad d(x, y) \geq 0. \tag{3.14a}$$

$$\text{Identity of indiscernibles:} \quad d(x, y) = 0 \Leftrightarrow x = y. \tag{3.14b}$$

$$\text{Symmetry:} \quad d(x, y) = d(y, x). \tag{3.14c}$$

$$\text{Triangle inequality:} \quad d(x, z) \leq d(x, y) + d(y, z). \tag{3.14d}$$

Single-object metrics

The Euclidean metric of order q between a state x and a corresponding estimate $\hat{x}$ is defined as

$$d_q(x, \hat{x}) = \|x - \hat{x}\|_q. \tag{3.15}$$

For performance evaluation of extended object estimates with ellipsoidal extents, a comparison study in [39] has shown that the Gaussian Wasserstein distance (GWD) is a good choice. The GWD between an extended object state $\xi = (x, X)$, where X is positive symmetric matrix used to represent the extent of an elliptic object, and a corresponding estimate $\hat{\xi} = \left(\hat{x}, \hat{X}\right)$ of order 2 is defined as [40]

$$d_{\mathrm{GW}}(\xi, \hat{\xi}) = \left(\|Hx - H\hat{x}\|_2^2 + \operatorname{trace}\left(X + \hat{X} - 2\left(X\hat{X}\right)^{\frac{1}{2}} \right) \right)^{\frac{1}{2}} \tag{3.16}$$

where the observation matrix H picks out the position from the kinematic state vector.

Multi-object metrics

In MOT, it is important to measure not only the state estimation error but also the cardinality estimation error due to misdetections and false detections. The different cardinality-related errors include

- Misdetections: true objects for which there are no corresponding estimates.

- False detections: object estimates for which there are no corresponding true objects.

An MOT metric computes the "distance" between a set of object states $\mathbf{x}$ and a corresponding set estimate $\hat{\mathbf{x}}$. It is assumed that a single object metric $d(x, \hat{x})$ is given. Further, let

$$d^{(c)}(x, \hat{x}) = \min(c; d(x, \hat{x})) \tag{3.17}$$

denote the distance cut-off at a distance $c > 0$ where c is a parameter.

OSPA

The Optimal Sub-Pattern Assignment (OSPA) multi-object metric is defined as [41], [42]

$$d_p^{(c)}(\mathbf{x}, \hat{\mathbf{x}}) = \begin{cases} \left(\frac{1}{|\hat{\mathbf{x}}|} \left(\min_{\pi \in \Pi_{|\hat{\mathbf{x}}|}} \sum_{i=1}^{|\mathbf{x}|} d^{(c)} \left(x_i, \hat{x}_{\pi(i)} \right)^p + c^p \left(|\hat{\mathbf{x}}| - |\mathbf{x}| \right) \right) \right)^{\frac{1}{p}} & \text{if } |\hat{\mathbf{x}}| \geq |\mathbf{x}| \\ \left(\frac{1}{|\mathbf{x}|} \left(\min_{\pi \in \Pi_{|\mathbf{x}|}} \sum_{i=1}^{|\hat{\mathbf{x}}|} d^{(c)} \left(\hat{x}_i, x_{\pi(i)} \right)^p + c^p \left(|\mathbf{x}| - |\hat{\mathbf{x}}| \right) \right) \right)^{\frac{1}{p}} & \text{if } |\hat{\mathbf{x}}| < |\mathbf{x}| \end{cases} \tag{3.18}$$

where $c > 0$, $1 \leq p < \infty$ and Π_i is the set of permutations of the set of integers $\{1, \ldots, i\}$ for any $i \in \mathbb{N}$ and for any element $\pi \in \Pi_i$ be a sequence $(\pi(1), \ldots, \pi(i))$. The parameter p determines the severity of penalizing the outliers in the localization component. The OSPA metric (for the case $|\hat{\mathbf{x}}| \geq |\mathbf{x}|$) can be decomposed into two parts:

- Normalized sum of state errors: $\frac{1}{|\hat{\mathbf{x}}|} \sum_{i=1}^{|\mathbf{x}|} d^{(c)} \left(x_i, \hat{x}_{\pi(i)} \right)^p$.
- Normalized cardinality error: $\frac{1}{|\hat{\mathbf{x}}|} c^p (|\hat{\mathbf{x}}| - |\mathbf{x}|)$.

GOSPA

The OSPA metric only accounts for localization error for the objects in the smallest set and cardinality mismatch; this is not desired in traditional MOT performance evaluation. For example, OSPA does not encourage trackers to have as few misdetections and false detections as possible. As a solution to this, the generalized OSPA (GOSPA) multi-object metric was proposed in

[43], which is able to penalize localization errors for properly detected objects, misdetections and false detection. The GOSPA metric is defined as

$$d_p^{(c,\alpha)}(\mathbf{x},\hat{\mathbf{x}}) = \begin{cases} \left(\min_{\pi\in\Pi_{|\mathbf{x}|}} \sum_{i=1}^{|\mathbf{x}|} d^{(c)}\left(x_i,\hat{x}_{\pi(i)}\right)^p + \frac{c^p}{\alpha}(|\hat{\mathbf{x}}|-|\mathbf{x}|)\right)^{\frac{1}{p}} & \text{if } |\hat{\mathbf{x}}|\geq|\mathbf{x}| \\ \left(\min_{\pi\in\Pi_{|\mathbf{x}|}} \sum_{i=1}^{|\hat{\mathbf{x}}|} d^{(c)}\left(\hat{x}_i,x_{\pi(i)}\right)^p + \frac{c^p}{\alpha}(|\mathbf{x}|-|\hat{\mathbf{x}}|)\right)^{\frac{1}{p}} & \text{if } |\hat{\mathbf{x}}|<|\mathbf{x}| \end{cases} \tag{3.19}$$

where $c>0$, $1\leq p<\infty$ and $0<\alpha\leq 2$.

Compared to the OSPA metric (3.18), there is no normalization factor $\max(|\mathbf{x}|,|\hat{\mathbf{x}}|)$ and an additional parameter α has been introduced. Setting $\alpha=1$ gives the OSPA metric without normalization. Moreover, it has been shown in [44] that the spooky effect arises in optimal estimation of multiple objects with the OSPA metric; however, this is not the case for the GOSPA metric.

When the GOSPA metric is used for MOT performance evaluation to measure the "distance" between the true set of object states $\mathbf{x}$ and the estimated set of object states $\hat{\mathbf{x}}$, it is most appropriate to set $\alpha=2$. In this case, the GOSPA metric can be re-written as

$$d_p^{(c,2)}(\mathbf{x},\hat{\mathbf{x}}) = \left(\min_{\theta\in\Theta^{(|\mathbf{x}|,|\hat{\mathbf{x}}|)}} \sum_{(i,j)\in\theta} d^{(c)}\left(x^i,\hat{x}^j\right)^p + \frac{c^p}{2}(|\mathbf{x}|-|\theta|+|\hat{\mathbf{x}}|-|\theta|)\right)^{\frac{1}{p}} \tag{3.20}$$

where $\Theta^{(|\mathbf{x}|,|\hat{\mathbf{x}}|)}$ is the set of all possible 2D assignments. An assignment set θ between the sets $\{1,\ldots,|\mathbf{x}|\}$ and $\{1,\ldots,|\hat{\mathbf{x}}|\}$ is a set that has the following properties: $\theta\subseteq\{1,\ldots,|\mathbf{x}|\}\times\{1,\ldots,|\hat{\mathbf{x}}|\}$, $(i,j),(i,j')\in\theta\Rightarrow j=j'$ and $(i',j),(i,j)\in\theta\Rightarrow i=i'$ where the last two properties ensure that every i and j gets at most one assignment. Equation (3.20) facilitates the decomposition of the GOSPA metric into three parts:

- Sum of state errors: $\sum_{(i,j)\in\theta} d^{(c)}\left(x^i,\hat{x}^j\right)^p$.
- Misdetection error: $\frac{c^p}{2}(|\mathbf{x}|-|\theta|)$
- False detection error: $\frac{c^p}{2}(|\hat{\mathbf{x}}|-|\theta|)$.

CHAPTER 4

Multi-object modeling

The formulation of an MOT problem needs systematic formal modeling for multi-object dynamics and measurements. This chapter introduces the multi-object dynamic and measurement models used in this thesis.

4.1 Multi-object dynamic model

Multi-object dynamic models should include models for the motion of individual objects as well as models for object appearance and disappearance to handle an unknown and time-varying number of objects. In MOT literature, object appearance and disappearance are often referred to as object birth and death, respectively. The multi-object dynamic model $p(\mathbf{x}_{k+1}|\mathbf{x}_k)$ used in this thesis is based on the following assumptions:

- Single object with state x_k at time step k moves to a new state x_{k+1} at time step $k+1$ with a Markov transition density $\pi_k(x_{k+1}|x_k)$.

- A single object with state x_k at time step k has a probability $P^S(x_k)$ of surviving into time step $k+1$.

- The RFS of objects at time step $k+1$ is the union of the RFS of objects that survive from time step k to time step $k+1$, denoted $\mathbf{x}_{k+1}^{S}$, and the RFS of newborn objects, denoted $\mathbf{x}_{k+1}^{B}$,

$$\mathbf{x}_{k+1} = \mathbf{x}_{k+1}^{S} \cup \mathbf{x}_{k+1}^{B}. \tag{4.1}$$

- Object birth, object death, and object motion are conditionally independent of the previous multi-object state.

Birth models

The common RFS models for object birth include a model for the number of objects expected to be born, i.e., a birth cardinality distribution, and a model for the states of the newborn objects, i.e., a birth state density. In many cases, a new object can appear anywhere in the surveillance area, so it is important to use a spatial distribution that covers the entire area. In some cases, objects may only be born in specific areas, and it is then more suitable to use a spatial distribution localized to those areas.

Poisson birth model

To model the number of new objects that appear at a time step as being Poisson distributed is the most common choice in MOT. When using RFSs to model MOT, a Poisson number of new objects means that the object birth is modeled as a Poisson RFS. For a Poisson birth model, at time step k a possibly empty set of newborn objects $\mathbf{x}_k^B$ appears, distributed according to a Poisson RFS with intensity $\lambda_k^B(x_k)$. That the set is possibly empty means that it is possible that no object is born at all.

The birth cardinality distribution is Poisson, with parameter $\bar{\lambda}_k^B$,

$$\rho(n_k^B = j) = e^{-\bar{\lambda}_k^B} \frac{\left(\bar{\lambda}_k^B\right)}{j!} \tag{4.2}$$

where

$$\bar{\lambda}_k^B = \int \lambda_k^B dx_k \tag{4.3}$$

and the expected number of births is $\bar{\lambda}_k^B$. For a non-empty set of new objects,

their states are independent and identically distributed (i.i.d.) with density

$$\frac{\lambda_k^B(x_k)}{\bar{\lambda}_k^B}. \tag{4.4}$$

The most common representation of the Poisson RFS birth intensity is an un-normalized density mixture,

$$\lambda_k^B(x_k) = \sum_{i=1}^{N_k^B} w_k^{B,i} p_k^{B,i}(x_k). \tag{4.5}$$

With a mixture intensity, the Poisson RFS birth parameters are the set of weights and densities,

$$\left\{ \left(w_k^{B,i}, p_k^{B,i}(\cdot) \right) \right\}_{i=1}^{N_k^B}. \tag{4.6}$$

For Gaussian models, it is suitable to let the Poisson RFS intensity be a Gaussian mixture,

$$\lambda_k^B(x_k) = \sum_{i=1}^{N_k^B} w_k^{B,i} \mathcal{N}\left(x_k; \bar{x}_k^{B,i}, P_k^{B,i} \right). \tag{4.7}$$

Bernoulli and multi-Bernoulli birth models

Object birth models can be also built upon Bernoulli RFSs. For a Bernoulli birth model, at time step k an object is born with probability r_k^B (i.e., no object with probability $1 - r_k^B$), and if an object is born, the initial object state x_k has density $p_k^B(x_k)$. In a Bernoulli birth model, the probability of birth r_k^B gives the birth cardinality distribution, which is a Bernoulli,

$$\rho(n_k^B = j) = \begin{cases} 1 - r_k^B & \text{if } j = 0 \\ r_k^B & \text{if } j = 1 \\ 0 & \text{otherwise} \end{cases} \tag{4.8}$$

where n_k^B denotes the number of births at time step k.

It is more general to use an MB birth model, which is the union of independent Bernoulli births. The parameters of an MB birth are the set of Bernoulli

birth parameters,

$$\left\{\left(r_k^{B,i}, p_k^{B,i}(\cdot)\right)\right\}_{i=1}^{N_k^B}. \tag{4.9}$$

For an MB birth model, the expected number of births is given by the sum of the probabilities of birth $\sum_{i=1}^{N_k^B} r_k^{B,i}$. The MB birth cardinality distribution is given by the convolution of the Bernoulli birth cardinality distributions. In case $r_k^{B,i} = r$ for all i, then the birth cardinality distribution is a Binomial,

$$\rho(n_k^B = j) = \begin{cases} \binom{n_k^B}{j} r^j (1-r)^{n_k^B - j} & \text{if } n_k^B = 0, 1, \ldots, N_k^B \\ 0 & \text{if } n_k^B > N_k^B. \end{cases} \tag{4.10}$$

Compared to the Poisson birth model, the MB birth model bounds a priori the number of objects that can appear in the surveillance area. For linear and Gaussian models, it is suitable to let the Bernoulli birth densities be Gaussian,

$$p_k^{B,i}(x_k) = \mathcal{N}(x_k; \bar{x}_k^{B,i}, P_k^{B,i}). \tag{4.11}$$

Single-object dynamic models

This section introduces two common 2D single-object dynamic models used in this thesis. A survey of dynamic models for object tracking is given in [45].

Nearly constant velocity model

The single object state is $x = [p_x, v_x, p_y, v_y]^{\mathrm{T}}$ where $[p_x, p_y]^{\mathrm{T}}$ is the position vector and $[v_x, v_y]^{\mathrm{T}}$ is the velocity vector. The single object state transition density from the object state x to the object state y at the next time step is

$$\pi(y|x) = \mathcal{N}(y; Fx, Q) \tag{4.12}$$

where

$$F = I_2 \otimes \begin{bmatrix} 1 & T \\ 0 & 1 \end{bmatrix}, \tag{4.13a}$$

$$Q = \sigma_v^2 I_2 \otimes \begin{bmatrix} T^3/3 & T^2/2 \\ T^2/2 & T \end{bmatrix}. \tag{4.13b}$$

Here T is the sampling time, $\sigma_{\dot{v}}$ is a parameter controlling the process noise level and I_n is the identity matrix of size n.

Coordinate turn model with polar velocity

The single object state is $x = [p_x, p_y, v, \phi, \omega]^{\mathrm{T}}$ where $[p_x, p_y]^{\mathrm{T}}$ is the position vector, v is the polar velocity, ϕ is the heading and ω is the turn rate. By linearization first and then discretization, the relation between the object state x at the current time step and the object state y at the next time step can be written as

$$y = \begin{bmatrix} p_x + (2v/\omega)\sin(\omega T/2)\cos(\phi + \omega T/2) \\ p_y + (2v/\omega)\sin(\omega T/2)\sin(\phi + \omega T/2) \\ v \\ \phi + \omega T \\ \omega \end{bmatrix} + w \tag{4.14}$$

where w is white noise with covariance

$$Q = \mathrm{blkdiag}\left(\begin{bmatrix} 0 & 0 \\ 0 & 0 \end{bmatrix}, T^2\sigma_{\dot{v}}^2, \begin{bmatrix} T^3/3 & T^2/2 \\ T^2/2 & T \end{bmatrix}\sigma_{\dot{\omega}}^2\right) \tag{4.15}$$

where blkdiag denotes block diagonalization, and $\sigma_{\dot{v}}^2$ and $\sigma_{\dot{\omega}}^2$ are parameters controlling the process noise level.

4.2 Multi-object measurement model

Multi-object measurement models should include models for the measurements originating from individual objects as well as models for clutter measurements, i.e., measurements not originating from objects. This section introduces the (single-sensor) multi-object measurement models $p(\mathbf{z}_k|\mathbf{x}_k)$ for both point and extended objects. The two measurement models are based on the following common assumptions:

- The measurement set $\mathbf{z}_k$ at time step k is an RFS consisting of the RFS $\mathbf{z}_k^O(\mathbf{x}_k)$ of measurements generated by the set of objects with states $\mathbf{x}_k$ and the RFS $\mathbf{z}_k^C$ of clutter measurements, i.e.,

$$\mathbf{z}_k = \mathbf{z}_k^O(\mathbf{x}_k) \cup \mathbf{z}_k^C. \tag{4.16}$$

- The RFSs $\mathbf{z}_k^O(\mathbf{x}_k)$ and $\mathbf{z}_k^C$ are statistically independent.
- No measurement is generated by more than one object.
- Given a set $\mathbf{x}_k$ of objects, each object $x \in \mathbf{x}_k$ is either detected with probability $P^D(x)$ and generates a set of measurements $\mathbf{z}^O(x)$ with conditional density $g(\mathbf{z}^O(x)|x)$, or missed with probability $1 - P^D(x)$.
- The RFS $\mathbf{z}^O$ is a Poisson RFS with intensity $\lambda^C(\cdot)$.

Point objects

In point object tracking, each object generates at most a single measurement per time step, i.e., a single resolution cell is occupied by an object. In this case, $|\mathbf{z}^O(x)| \leq 1$.

Extended objects

In EOT, each object may generate multiple measurements per time step and the measurements are spatially distributed around the objects, i.e., multiple resolution cells are occupied by an object. In this case, the object-generated measurements $\mathbf{z}^O(x)$ are typically modeled by a Poisson RFS. This models the number of detections as $|\mathbf{z}^O(x)|$ Poisson distributed with a rate $\lambda^O(x)$ that is a function of the object state x. The single-object measurement likelihood for an extended object is

$$p(\mathbf{z}^O(x)|x) = e^{-\lambda^O(x)} \lambda^O(x)^{|\mathbf{z}^O(x)|} \prod_{z \in \mathbf{z}^O(x)} g(z|x). \tag{4.17}$$

CHAPTER 5

Multi-object conjugate priors for multi-object tracking

Due to the unknown correspondence between measurements and object states, MOT is combinatorial in nature, and thus is highly computationally demanding. MOT conjugate priors are one tool for managing complexity, by exploiting forms which maintain structure through prediction and update steps. This chapter introduces single-object and multi-object conjugacy used in this thesis.

5.1 Conjugate prior

If $\mathscr{L}$ is a class of measurement likelihoods $g(z|x)$, and $\mathscr{F}$ is a class of prior distributions for x, then the class $\mathscr{F}$ is conjugate for $\mathscr{L}$ if

$$p(x|z) \in \mathscr{F} \ \forall \ g(z|x) \in \mathscr{L} \text{ and } p(x) \in \mathscr{F}. \tag{5.1}$$

Many examples of conjugate priors can be found from the exponential family of distributions. In each of these cases, the posterior has the same form with the same number of parameters as the prior.

Another common structure is when the prior family contains mixtures of

distributions of a given form. Let $\bar{\mathscr{F}}$ denote the family of mixtures of distributions in $\mathscr{F}$, and let $\bar{\mathscr{L}}$ denote the family of mixtures of likelihoods in $\mathscr{L}$. It can be shown that, if $\mathscr{F}$ is a conjugate prior for the measurement likelihood $\mathscr{L}$, then $\bar{\mathscr{F}}$ is also conjugate prior for $\mathscr{L}$, and the posterior will contain the same number of mixture components as the prior. Further, $\bar{\mathscr{F}}$ is also conjugate prior for $\bar{\mathscr{L}}$, but the number of mixture components in the posterior will be the product of the number of components in the prior and in the measurement likelihood. In this case, the posterior is in the same form, but the complexity of the representation grows and eventually approximation becomes necessary. Many examples of this kind can be found in (multiple) object tracking in clutter.

5.2 Single-object conjugate prior

If $\mathscr{L}$ is a class of measurement likelihoods $g_k(z_k|x_k)$, $\mathscr{T}$ is a class of transition densities $\pi_k(x_k|x_{k-1})$, and $\mathscr{F}$ is a class of single-object densities for x, then the class $\mathscr{F}$ is single-object conjugate for $\mathscr{L}$ and $\mathscr{T}$ if

$$p(x_k|z_{1:k-1}) \in \mathscr{F} \;\forall\; \pi_k(x_k|x_{k-1}) \in \mathscr{T} \text{ and } p(x_{k-1}|z_{1:k-1}) \in \mathscr{F}, \tag{5.2}$$

$$p(x_k|z_{1:k}) \in \mathscr{F} \;\forall\; g_k(z_k|x_k) \in \mathscr{L} \text{ and } p(x_k|z_{1:k-1}) \in \mathscr{F}. \tag{5.3}$$

Single-object conjugate prior can be understood as a generalization of conjugacy, which originally only concerns Bayes update, to the whole filtering recursion.

Gaussian conjugate prior

Single point object tracking typically concerns the following Bayesian filtering recursions:

$$p\left(x_k|z_{1:k}\right) = \frac{g_k\left(z_k|x_k\right) p\left(x_k|z_{1:k-1}\right)}{\int g_k\left(z_k|x'_k\right) p\left(x'_k|z_{1:k-1}\right) dx'_k}, \tag{5.4}$$

$$p\left(x_k|z_{1:k-1}\right) = \int \pi_k\left(x_k|x_{k-1}\right) p\left(x_{k-1}|z_{1:k-1}\right) dx_{k-1}. \tag{5.5}$$

The Kalman filter and the EKF, introduced in Section 2.2, are two examples of single-object filters based on single-object conjugate prior where both the

predicted density and the posterior density are Gaussian.

Gamma Gaussian inverse-Wishart conjugate prior

For EOT using the Poisson spatial model and the random matrix approach, the objects are assumed to have elliptic shapes, and the Bayesian filtering recursions are

$$p(\xi_k|\mathbf{z}_{1:k}) = \frac{p(\mathbf{z}_k|\xi_k)p(\xi_k|\mathbf{z}_{1:k-1})}{\int p(\mathbf{z}_k|\xi_k)p(\xi_k|\mathbf{z}_{1:k-1})d\xi_k}, \tag{5.6}$$

$$p(\xi_k|\mathbf{z}_{1:k-1}) = \int \pi_k(\xi_k|\xi_{k-1})p(\xi_{k-1}|\mathbf{z}_{1:k-1})d\xi_{k-1} \tag{5.7}$$

where $\xi_k = (\gamma_k, x_k, X_k)$ is a combination of a Poisson rate γ_k, a kinematic state vector x_k and an extent matrix X_k. Various random matrix approaches with different prediction and update steps have been proposed in the literature; see [4, Section III.A] for an overview. Here the random matrix approach with improved noise modeling proposed in [46] is taken as an example to motivate the use of a gamma Gaussian inverse-Wishart (GGIW) conjugate prior in EOT.

For the improved noise modeling with the number of measurements being Poisson, the measurement likelihood can be factorized as

$$p(\mathbf{z}_k|\xi_k) = e^{-\gamma_k}\gamma_k^{|\mathbf{z}_k|}\prod_{z_k\in\mathbf{z}_k}\mathcal{N}(z_k; H_k x_k, \rho X_k + R_k) \tag{5.8}$$

where ρ is a scaling factor and R_k is the measurement noise covariance matrix. The Bayesian conjugate prior for an unknown Poisson rate is the gamma distribution. Also, for Gaussian measurements, the conjugate priors for unknown mean and covariance are the Gaussian and the inverse-Wishart distributions, respectively. This motivates the use of a GGIW representation for the object state density,

$$p(\xi_k|\mathbf{z}_{1:k}) = \mathcal{G}(\gamma_k; \alpha_{k|k}, \beta_{k|k})\mathcal{N}(x_k; \bar{x}_{k|k}, P_{k|k})\mathcal{IW}(X_k; \nu_{k|k}, V_{k|k}). \tag{5.9}$$

For a GGIW prior of the form (5.9), and a measurement likelihood of the form (5.8), the measurement update (5.6) is not analytically tractable; however, the filtering density $p(\xi_k|\mathbf{z}_{1:k})$ can still be approximated as a GGIW. The

approximate update can be based on either the approximation of non-linear functions of the extent using matrix square roots [46] or variational Bayesian approximation [47].

The GGIW conjugacy also holds for the prediction step. Though no closed form solution exists for a Wishart transition density of the extent matrix, the predicted density (5.7) can be approximated as a GGIW by either applying a simple heuristic or minimizing the Kullback-Leibler divergence (KLD) [48].

5.3 Multi-object conjugate prior

If $\mathscr{L}$ is a class of multi-object measurement likelihoods $p(\mathbf{z}_k|\mathbf{x}_k)$, $\mathscr{T}$ is a class of multi-object transition densities $p(\mathbf{x}_k|\mathbf{x}_{k-1})$, and $\mathscr{F}$ is a class of multi-object densities for $\mathbf{x}$, then the class $\mathscr{F}$ is multi-object conjugate for $\mathscr{L}$ and $\mathscr{T}$ if

$$p(\mathbf{x}_k|\mathbf{z}_{1:k-1}) \in \mathscr{F} \ \forall \ p(\mathbf{x}_k|\mathbf{x}_{k-1}) \in \mathscr{T} \text{ and } p(\mathbf{x}_{k-1}|\mathbf{z}_{1:k-1}) \in \mathscr{F}, \tag{5.10}$$

$$p(\mathbf{x}_k|\mathbf{z}_{1:k}) \in \mathscr{F} \ \forall \ p(\mathbf{z}_k|\mathbf{x}_k) \in \mathscr{L} \text{ and } p(\mathbf{x}_k|\mathbf{z}_{1:k-1}) \in \mathscr{F}. \tag{5.11}$$

Multi-object conjugacy is a generalization of the single-object conjugacy to consider the multi-object prediction and update,

$$p(\mathbf{x}_k|\mathbf{z}_{1:k-1}) = \int p(\mathbf{x}_k|\mathbf{x}_{k-1}) p(\mathbf{x}_{k-1}|\mathbf{z}_{1:k-1}) \delta\mathbf{x}_{k-1}, \tag{5.12}$$

$$p\left(\mathbf{x}_k|\mathbf{z}_{1:k}\right) = \frac{p\left(\mathbf{z}_k|\mathbf{x}_k\right) p\left(\mathbf{x}_k|\mathbf{z}_{1:k-1}\right)}{\int p\left(\mathbf{z}_k|\mathbf{x}'_k\right) p\left(\mathbf{x}'_k|\mathbf{z}_{1:k-1}\right) \delta\mathbf{x}'_k}. \tag{5.13}$$

Multi-object conjugacy is important for designing MOT algorithms. With the use of multi-object conjugacy, it is convenient to

- express the theoretically exact density (for the given models),
- describe which parameters are needed to represent the density,
- find computationally tractable approximations, and
- analyze the approximation error.

For the multi-object models introduced in Chapter 4, there are two known classes of multi-object conjugate priors for both point and extended objects: the MBM densities [16], [20], [22] for MB birth model and the Poisson MBM (PMBM) densities [17]–[19] for Poisson birth model.

Multi-Bernoulli mixture conjugate prior

For MB(M) birth, the MBM density $\mathcal{MBM}_{k|k}(\mathbf{x}_k)$ is a multi-object conjugate prior to the multi-object transition density $p(\mathbf{x}_k|\mathbf{x}_{k-1})$ and measurement model $p(\mathbf{z}_k|\mathbf{x}_k)$ [20]. In other words, if the posterior density at time step $k-1$ is MBM, then the predicted density at time step k is MBM,

$$\mathcal{MBM}_{k|k-1}(\mathbf{x}_k) = \int p(\mathbf{x}_k|\mathbf{x}_{k-1})\mathcal{MBM}_{k-1|k-1}(\mathbf{x}_{k-1})\delta\mathbf{x}_{k-1}. \tag{5.14}$$

Further, if the prior density at time step k is MBM, then the Bayes posterior at time step k is MBM,

$$\mathcal{MBM}_{k|k}\left(\mathbf{x}_k\right) = \frac{p\left(\mathbf{z}_k|\mathbf{x}_k\right)\mathcal{MBM}_{k|k-1}\left(\mathbf{x}_k\right)}{\int p\left(\mathbf{z}_k|\mathbf{x}'_k\right)\mathcal{MBM}_{k|k-1}\left(\mathbf{x}'_k\right)\delta\mathbf{x}'_k}. \tag{5.15}$$

The MBM density is defined as

$$\mathcal{MBM}_{k|k}(\mathbf{x}_k) = \sum_{h_k=1}^{\mathcal{H}_k} w_{k|k}^{h_k}\mathcal{MB}_{k|k}^{h_k}\left(\mathbf{x}_k\right) \tag{5.16a}$$

$$= \sum_{h_k=1}^{\mathcal{H}_k} w_{k|k}^{h_k} \sum_{\uplus\mathbf{x}_k^i=\mathbf{x}_k} \prod_{i=1}^{N_k^{h_k}} \mathcal{B}_{k|k}^{i,h_k}\left(\mathbf{x}_k^i\right) \tag{5.16b}$$

where $\mathcal{MB}(\mathbf{x})$ and $\mathcal{B}(\mathbf{x})$ denote multi-Bernoulli density and Bernoulli density. Each global hypothesis h_k corresponds to a sequence of data associations, $\mathcal{H}_k$ denotes the number of global hypotheses, and the weight $w_{k|k}^{h_k}$ is the probability of the global hypothesis. The MBM density is fully parameterized by the parameters,

$$\left\{\left(w_{k|k}^{h_k}, \left\{\left(r_{k|k}^{i,h_k}, p_{k|k}^{i,h_k}(\cdot)\right)\right\}_{i=1}^{N_k^{h_k}}\right)\right\}_{h_k=1}^{\mathcal{H}_k}. \tag{5.17}$$

Predicting (5.14) and updating (5.15) the MBM density then comes down to computing the predicted and updated parameters.

The MBM filter is an MOT algorithm based on the MBM conjugate prior and consists of four building blocks: 1) prediction, 2) update, 3) reduction, and 4) estimation. A block-diagram for the MBM filter is presented in Fig.

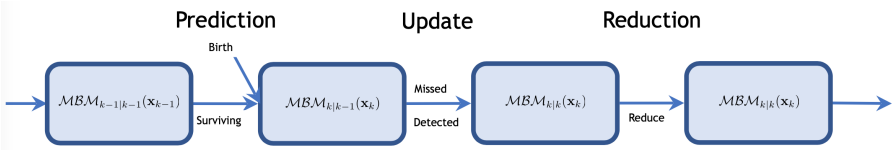

Figure 5.1: MBM filter block diagram

5.1. MBM reduction typically consists of 1) pruning MBs with low weights and 2) pruning Bernoullis with low probability of existence. The reader is referred to [20] for explicit equations and implementation details of the MBM filter. The MBM_{01} filter is based on the MBM_{01} conjugate prior. It has the same filtering recursion as the MBM filter but performs MBM_{01} expansion after the prediction step. This results in an exponential increase in number of global hypotheses in the MBM_{01} filter. The δ-generalized labeled multi-Bernoulli (δ-GLMB) filter [21], [22] is equivalent to the labeled MBM_{01} filter where labels are used for sequential track formation.

Poisson multi-Bernoulli mixture conjugate prior

With a Poisson birth, the PMBM density $\mathcal{PMBM}_{k|k}(\mathbf{x}_k)$ is a multi-object conjugate prior to the standard models [17], [18]. If the posterior at time step $k-1$ is PMBM, then for the multi-object transition density $p(\mathbf{x}_k|\mathbf{x}_{k-1})$ the predicted multi-object density is also PMBM,

$$\mathcal{PMBM}_{k|k-1}(\mathbf{x}_k) = \int p(\mathbf{x}_k|\mathbf{x}_{k-1})\,\mathcal{PMBM}_{k-1|k-1}(\mathbf{x}_{k-1})\,\delta\mathbf{x}_{k-1}. \quad (5.18)$$

Further, if the predicted multi-object density at time step k is PMBM, then for the multi-object measurement model $p(\mathbf{z}_k|\mathbf{x}_k)$ the Bayes posterior is also PMBM

$$\mathcal{PMBM}_{k|k}(\mathbf{x}_k) = \frac{p(\mathbf{z}_k|\mathbf{x}_k)\,\mathcal{PMBM}_{k|k-1}(\mathbf{x}_k)}{\int p(\mathbf{z}_k|\mathbf{x}'_k)\,\mathcal{PMBM}_{k|k-1}(\mathbf{x}'_k)\,\delta\mathbf{x}'_k}. \quad (5.19)$$

When using the PMBM conjugate prior for MOT, the set of objects $\mathbf{x}_k$ at time step k is the union of detected objects and undetected objects, i.e., $\mathbf{x}_k = \mathbf{x}_k^d \uplus \mathbf{x}_k^u$. The set of detected objects $\mathbf{x}_k^d$ consists of objects that the sensors have detected at least once. The set of undetected objects $\mathbf{x}_k^u$ consists

of objects that have never been detected by any of the sensors (but that are within the surveillance region of the sensors).

The PMBM density is defined as

$$\mathcal{PMBM}_{k|k}\left(\mathbf{x}_k\right) = \sum_{\mathbf{x}_k^u \uplus \mathbf{x}_k^d = \mathbf{x}_k} \mathcal{P}_{k|k}^u\left(\mathbf{x}_k^u\right) \mathcal{MBM}_{k|k}^d\left(\mathbf{x}_k^d\right) \tag{5.20}$$

with a PPP density $\mathcal{P}_{k|k}^u(\cdot)$ for undetected objects, and an MBM density $\mathcal{MBM}_{k|k}^d(\cdot)$ for detected objects. The undetected PPP intensity is typically an un-normalized density mixture,

$$\lambda_{k|k}^{\mathrm{u}}\left(x_k\right) = \sum_{t=1}^{N_k^{\mathrm{u}}} \tilde{w}_{k|k}^{\mathrm{u},t} p_{k|k}^{\mathrm{u},t}\left(x_k\right), \tag{5.21}$$

whose parameters are

$$\left\{\left(\tilde{w}_{k|k}^{\mathrm{u},t}, p_{k|k}^{\mathrm{u},t}(\cdot)\right)\right\}_{t=1}^{N_k^{\mathrm{u}}}. \tag{5.22}$$

The MBM density, defined in (5.16), for detected objects has parameters,

$$\left\{\left(w_{k|k}^{h_k}, \left\{\left(r_{k|k}^{i,h_k}, p_{k|k}^{i,h_k}(\cdot)\right)\right\}_{i=1}^{N_k^{h_k}}\right)\right\}_{h_k=1}^{\mathcal{H}_k}. \tag{5.23}$$

Therefore the PMBM density is fully parameterized by the parameters,

$$\left\{\left(\tilde{w}_{k|k}^{\mathrm{u},t}, p_{k|k}^{\mathrm{u},t}(\cdot)\right)\right\}_{t=1}^{N_k^{\mathrm{u}}}, \left\{\left(w_{k|k}^{h_k}, \left\{\left(r_{k|k}^{i,h_k}, p_{k|k}^{i,h_k}(\cdot)\right)\right\}_{i=1}^{N_k^{h_k}}\right)\right\}_{h_k=1}^{\mathcal{H}_k}. \tag{5.24}$$

A PMBM becomes an MBM if the intensity of the PPP is zero.

The PMBM density captures relevant uncertainties in MOT in an elegant way. In MOT the number of objects is unknown, and in the PMBM density this is captured by both the Bernoulli probabilities of existence, and by the undetected PPP intensity. The uncertainty about the object states are captured by the Bernoulli state densities for detected objects, and by the PPP intensity for undetected objects. Lastly, the unknown data association in MOT is captured by the MB mixture, where each mixture component corresponds to a sequence of (global) data associations, and the component weights are the

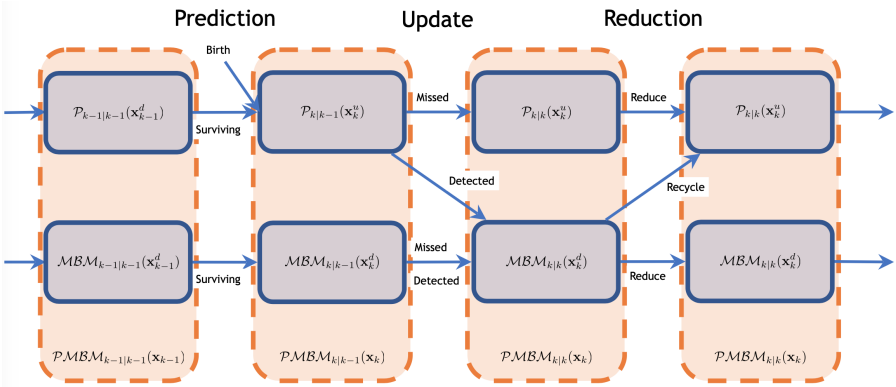

Figure 5.2: PMBM filter block diagram

estimated probability of the corresponding global associations.

The PMBM filter is an MOT algorithm based on the PMBM conjugate prior. The PMBM filter has a hypothesis structure in analogy to MHT, see, e.g., [25], [49] for detailed discussions. Similar to the MBM filter, the PMBM filter also consists of four building blocks: 1) prediction, 2) update, 3) reduction, and 4) estimation. A block-diagram for the PMBM filter is presented in Fig. 5.1. Here recycling means that Bernoullis with low probability of existence are approximated as a PPP and added to the PPP for undetected objects [50]. Compared to Bernoulli pruning, the information contained in the Bernoullis can be approximately retained in the PPP via recycling. The reader is referred to [17]–[19] for explicit equations and implementation details of the PMBM filter. The PMBM filter has a more efficient representation of the hypotheses than the MBM filter, thanks to the fact that the initiation of new Bernoullis is measurement-driven. Comparisons of MBM and PMBM filters have shown that, in terms of computational cost and estimation error, PMBM filter have better performance, see, e.g., [19], [20], [51], [52].

It is also useful to consider a PMB approximation to the PMBM density (5.20), which offers a trade-off between computational complexity and estimation performance. The PMB filter is a computationally efficient approximation of the PMBM filter by performing the PMB approximation after each update. Various PMB approximation methods exist for both point and extended objects [49], [53], [54], among which the one based on variational approximation

[53], [54] has the best performance when objects move in close proximity.

CHAPTER 6

Multi-object tracking based on sets of trajectories

In RFS-based algorithms for MOT, the main focus has been on the filtering problem. The object state estimation can be easily extracted from the multi-object filtering densities; however, it is not obvious how to build trajectories in a sound manner. A full Bayesian approach to MOT should characterize the distribution of the trajectories given the measurements, as it contains all information about the trajectories. This can be attained by considering multi-object density functions in which objects are trajectories [28], referred to as multi-trajectory densities. This chapter briefly reviews basic concepts of sets of trajectories and PMBM conjugate priors for sets of trajectories. In addition, a metric on the space of finite sets of trajectories [55] is introduced for MOT performance evaluation in terms of trajectory estimation error.

6.1 Sets of trajectories

This section reviews the state representations of trajectories and the integration of trajectory densities. In addition, possible problem formulations of MOT based on sets of trajectories used in this thesis are introduced.

Single trajectory

A trajectory consists of a sequence of object states that can start at any time step and end at any time after it starts. Mathematically, a trajectory is represented as a variable $X = (t, x^{1:i})$ where t is the initial time step of the trajectory, i is its length, and $x^{1:i} = (x^1, \ldots, x^i)$ denotes a sequence of length i that contains the object states at consecutive time steps of the trajectory. If k is the current time step, $t + i - 1 < k$ means that the trajectory ended at time $t + i - 1$, and $t + i - 1 = k$ means that the trajectory is ongoing.

As a trajectory $(t, x^{1:i})$ exists from time step t to $t + i - 1$, variable $(t + i)$ belongs to the set,

$$I_{(k')} = \{(t, i) : 0 \leq t \leq k' < \infty \text{ and } 1 \leq i \leq k' - t + 1 < \infty\}. \tag{6.1}$$

A single trajectory X up to a finite time step k' therefore belongs to the space

$$\mathfrak{T}_{k'} = \uplus_{(t,i)\in I_{(k')}} \{t\} \times \mathfrak{X}^i \tag{6.2}$$

where $\mathfrak{X}^i$ represents i Cartesian products of single object state space $\mathfrak{X}$. Given a real-valued function $p(\cdot)$ on the single trajectory space $\mathfrak{T}_{(k')}$, its integral is

$$\int p(X)dX = \sum_{(t,i)\in I_{(k')}} \int p\left(t, x^{1:i}\right) dx^{1:i} \tag{6.3}$$

where single trajectory density $p(t, x^{1:i})$ can be factorized as

$$p(t, x^{1:i}) = p(x^{1:i}|t, i)P(t, i). \tag{6.4}$$

This integral goes through all possible start times, lengths, and object states of the trajectory.

Multiple trajectories

A set of trajectories up to a finite time step k' is denoted by $\mathbf{X} \in \mathcal{F}(\mathfrak{T}_{(k')})$ where $\mathcal{F}(\mathfrak{T}_{(k')})$ is the set of all the finite subsets of $\mathfrak{T}_{(k')}$. Given a trajectory

$X = (t, x^{1:i})$, the set of the object state at time step k is

$$\tau_k(X) = \begin{cases} \{x^{k+1-t}\} & \text{if } t \leq k \leq t+i-1 \\ \varnothing & \text{otherwise} \end{cases}. \tag{6.5}$$

A trajectory X is present at time step k if and only if $|\tau^k(X)| = 1$. Given a set $\mathbf{X}$ of trajectories, the set $\tau^k(\mathbf{X})$ of object states at time step k is

$$\tau^k(\mathbf{X}) = \bigcup_{X \in \mathbf{X}} \tau^k(X). \tag{6.6}$$

The number of trajectories present at time k is given by $|\tau^k(\mathbf{X})|$.

Given a real-valued function $f(\cdot)$ on the space $\mathcal{F}(\mathfrak{T}_{(k')})$ of sets of trajectories, its set integral is

$$\int f(\mathbf{X})\delta\mathbf{X} = \sum_{n=0}^{\infty} \frac{1}{n!} \int f\left(\{X_1, \ldots, X_n\}\right) dX_{1:n} \tag{6.7}$$

where $X_{1:n} = (X_1, \ldots, X_n)$. If $f(\cdot)$ is a multi-trajectory density, then $f(\cdot) \geq 0$ and its set integral is one.

Multi-trajectory processes are analogous to multi-object processes for sets of object. A trajectory Poisson RFS has density

$$f(\mathbf{X}) = e^{-\int \lambda(X) dX} \lambda^{\mathbf{X}} \tag{6.8}$$

where the trajectory Poisson intensity $\lambda(\cdot)$ is defined on the trajectory state space, i.e., realizations of the Poisson RFS are trajectories with a birth time, a length, and a state sequence. A trajectory Bernoulli RFS has density

$$f(\mathbf{X}) = \begin{cases} 1 - r & \text{if } \mathbf{X} = \varnothing \\ rp(X) & \text{if } \mathbf{X} = \{X\} \\ 0 & \text{otherwise} \end{cases} \tag{6.9}$$

where $p(\cdot)$ is a trajectory state density and r is the Bernoulli probability of existence. A trajectory MB is the disjoint union of multiple trajectory Bernoulli RFSs; trajectory MBM RFS is an RFS whose density is a mixture of trajectory MB densities.

Problem formulation

There are many ways in which an MOT problem can be formulated depending on the application at hand. In this thesis, the following two variants are considered:

- The set of current trajectories: the objective is to estimate the trajectories of the objects who are present in the surveillance area at the current time.

- The set of all trajectories: the objective is to estimate the trajectories of all objects that have passed through the surveillance area at some point between time step 0 and the current time step, i.e., both the objects that are present in the surveillance area at the current time, and the objects that have left the surveillance area (but were in the surveillance area at at least one previous time).

Depending on the problem formulation, the variable that we are interested in is different. For the set of current trajectories, $\mathbf{X}_k$ is the set of trajectories for which $t+i-1=k$. For the set of all trajectories, $\mathbf{X}_k$ is the set of trajectories for which $t+i-1 \leq k$.

With the set of trajectories $\mathbf{X}_k$ as variables of interest in MOT, the Bayesian filtering recursions are

$$p\left(\mathbf{X}_k|\mathbf{z}_{1:k-1}\right) = \int p\left(\mathbf{X}_k|\mathbf{X}_{k-1}\right) p\left(\mathbf{X}_{k-1}|\mathbf{z}_{1:k-1}\right) \delta\mathbf{X}_{k-1}, \tag{6.10}$$

$$p\left(\mathbf{X}_k|\mathbf{z}_{1:k}\right) = \frac{p\left(\mathbf{z}_k|\mathbf{X}_k\right) p\left(\mathbf{X}_k|\mathbf{z}_{1:k-1}\right)}{\int p\left(\mathbf{z}_k|\mathbf{X}'_k\right) p\left(\mathbf{X}'_k|\mathbf{z}_{1:k-1}\right) \delta\mathbf{X}'_k} \tag{6.11}$$

where $p(\mathbf{X}_k|\mathbf{X}_{k-1})$ and $p(\mathbf{z}_k|\mathbf{X}_k)$ are multi-object dynamic and measurement models for sets of trajectories, defined analogously to their counterparts for sets of objects in Chapter 4. See [28] for details.

6.2 PMBMs for sets of trajectories

This section introduces the PMBM conjugate prior for sets of trajectories [30], [56], [57]. It was shown in [30] that the PMBM multi-trajectory density $\mathcal{PMBM}_{k|k}(\mathbf{X}_k)$ is a conjugate prior to multi-object models with point objects

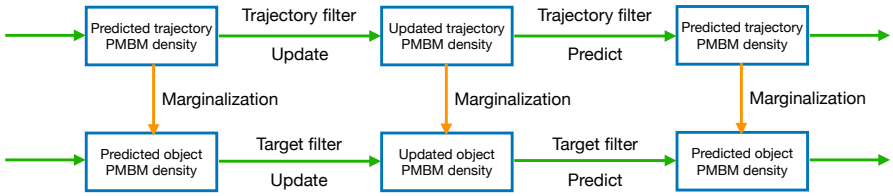

Figure 6.1: Trajectory PMBM filter versus object PMBM filter.

assumption and Poisson birth:

$$\mathcal{PMBM}_{k|k-1}(\mathbf{X}_k) = \int p(\mathbf{X}_k|\mathbf{X}_{k-1})\,\mathcal{PMBM}_{k-1|k-1}(\mathbf{X}_{k-1})\,\delta\mathbf{X}_{k-1}, \tag{6.12}$$

$$\mathcal{PMBM}_{k|k}(\mathbf{X}_k) = \frac{p(\mathbf{z}_k|\mathbf{X}_k)\,\mathcal{PMBM}_{k|k-1}(\mathbf{X}_k)}{\int p(\mathbf{z}_k|\mathbf{X}'_k)\,\mathcal{PMBM}_{k|k-1}(\mathbf{X}'_k)\,\delta\mathbf{X}'_k}. \tag{6.13}$$

In a PMBM multi-trajectory density, the trajectory Poisson RFS models trajectories of the set of undetected objects, whereas the trajectory MBM RFS models trajectories of objects that have been detected (in one of observed measurement sets). In a trajectory MBM, each Bernoulli RFS models a single potential trajectory given a sequence of associations, an MB RFS models a set of detected trajectories for a global hypothesis, and the weights of MBs are the estimated probability of the corresponding associations.

A trajectory Poisson/Bernoulli RFS density can be marginalized to the current time step to obtain an object Poisson/Bernoulli RFS density. Therefore marginalizing a PMBM set of trajectories density gives a PMBM set of object states density. The trajectory PMBM filter is an MOT algorithm based on the PMBM conjugate prior for sets of trajectories; see [30] for explicit equations and implementation details. The relation between a trajectory PMBM filter and an object PMBM filter is illustrated in Figure 6.1. Two key insights are: 1) in object PMBM filter the object state history is marginalized out in every prediction step, and 2) in trajectory PMBM filter information about the past object states is maintained such that trajectories can be estimated directly from the posterior.

6.3 Metric on the space of sets of trajectories

A metric for sets of trajectories based on multi-dimensional assignments was proposed in [55]. This metric penalizes localization costs for properly detected objects, misdetections, false detections and track switches. Let $\Pi_{\mathbf{X},\mathbf{Y}}$ be the set of all possible assignment vectors between the index sets $\{1\ldots,|\mathbf{X}|\}$ and $\{0,\ldots,|\mathbf{Y}|\}$. An assignment vector $\pi^k = [\pi_1^k,\ldots,\pi_{|\mathbf{X}|}^k]^{\mathrm{T}}$ at time step k is a vector $\pi^k \in \{0,\ldots,|\mathbf{Y}|\}^{n_\mathbf{X}}$ such that its ith component $\pi_i^k = \pi_{i'}^k = j > 0$ implies that $i = i'$. Here $\pi_i^k = j \neq 0$ implies that trajectory i in $\mathbf{X}$ is assigned to trajectory j in $\mathbf{Y}$ at time step k and $\pi_i^k = 0$ implies that trajectory i in $\mathbf{X}$ is unassigned at time step k.

For $1 \leq p < \infty$, cut-off parameter $c > 0$, switching penalty $\gamma > 0$ and a base metric $d_b(\cdot,\cdot)$ in the single object space $\mathfrak{X}$, the multi-dimensional assignment metric $d_p^{(c,\gamma)}(\mathbf{X},\mathbf{Y})$ between two sets $\mathbf{X}$ and $\mathbf{Y}$ of trajectories in time interval $1,\ldots,T$ is

$$d_p^{(c,\gamma)}(\mathbf{X},\mathbf{Y}) = \min_{\pi^k \in \Pi_{\mathbf{X},\mathbf{Y}}} \left(\sum_{k=1}^{T} d_{\mathbf{X},\mathbf{Y}}^k \left(\mathbf{X},\mathbf{Y},\pi^k\right)^p + \sum_{k=1}^{T-1} s_{\mathbf{X},\mathbf{Y}} \left(\pi^k,\pi^{k+1}\right)^p \right)^{\frac{1}{p}} \tag{6.14}$$

where the costs (to the p-th power) for properly detected objects, misdetections and false detections at time step k are

$$d_{\mathbf{X},\mathbf{Y}}^k \left(\mathbf{X},\mathbf{Y},\pi^k\right)^p = \sum_{(i,j)\in\theta^k(\pi^k)} d\left(\tau^k(X_i),\tau^k(Y_j)\right)^p + \frac{c^p}{2}\left(\left|\tau^k(\mathbf{X})\right| + \left|\tau^k(\mathbf{Y})\right| - 2\left|\theta^k\left(\pi^k\right)\right|\right) \tag{6.15}$$

with

$$\theta^k\left(\pi^k\right) = \left\{\left(i,\pi_i^k\right) : i \in \{1,\ldots,n_\mathbf{X}\},\ |\tau^k(X_i)| = \left|\tau^k(Y_{\pi_i^k})\right| = 1, d\left(\tau^k(X_i),\tau^k(Y_{\pi_i^k}) < c\right)\right\} \tag{6.16}$$

and the switching cost (to the p-th power) from time step k to $k+1$ is given

by

$$s_{\mathbf{X},\mathbf{Y}}(\pi^k, \pi^{k+1})^p = \gamma^p \sum_{i=1}^{|\mathbf{X}|} s\left(\pi_i^k, \pi_i^{k+1}\right) \tag{6.17}$$

$$s\left(\pi_i^k, \pi_i^{k+1}\right) = \begin{cases} 0 & \text{if } \pi_i^k = \pi_i^{k+1} \\ 1 & \text{if } \pi_i^k \neq \pi_i^{k+1}, \pi_i^k \neq 0, \pi_i^{k+1} \neq 0 \\ \frac{1}{2} & \text{otherwise} \end{cases}. \tag{6.18}$$

It should be noted that, for $(i,j) \in \theta^k$, $\tau^k(X_i)$ and $\tau^k(Y_{\pi_i^k})$ contain precisely one element and their distance is smaller than c, so $d\left(\tau^k(X_i), \tau^k(Y_j)\right)$ coincides with $d_b(\cdot,\cdot)$ evaluated at the corresponding single object states, which corresponds to the localization error. Therefore, (6.15) represents the sum of the costs (to the pth power) that correspond to localization error for properly detected objects (indicated by the assignments in $\theta^k(\pi^k)$), number of misdetections ($|\tau^k(\mathbf{X})| - |\theta^k(\pi^k)|$) and false detections ($|\tau^k(\mathbf{Y})| - |\theta^k(\pi^k)|$) at time step k.

The metric (6.14) can be computed by solving a multi-dimensional assignment problem, which may be computationally heavy for large T. It was further shown in [55] that an accurate lower bound on the metric (6.14) can be obtained using linear programming, which can be computed in polynomial time. Note that this lower bound is also a metric.

CHAPTER 7

Summary of included papers

This chapter provides a summary of the included papers.

7.1 Paper A

Yuxuan Xia, Karl Granström, Lennart Svensson,
Ángel F. García-Fernández, Jason L. Williams
Multi-scan implementation of the trajectory Poisson multi-Bernoulli mixture filter
Published in Journal of Advances in Information Fusion,
vol. 14, no. 2, pp. 213–235, Apr. 2019.
 ISBN: 1557-6418 .

The Poisson multi-Bernoulli mixture (PMBM) and the multi-Bernoulli mixture (MBM) are two multi-target distributions for which closed-form filtering recursions exist. The PMBM has a Poisson birth process, whereas the MBM has a multi-Bernoulli birth process. This paper considers a recently developed formulation of the multi-target tracking problem using a random finite set of trajectories, through which the track continuity is explicitly established. A

multi-scan trajectory PMBM filter and a multi-scan trajectory MBM filter, with the ability to correct past data association decisions to improve current decisions, are presented. In addition, a multi-scan trajectory MBM_{01} filter, in which the existence probabilities of all Bernoulli components are either 0 or 1, is presented. This paper proposes an efficient implementation that performs track-oriented N-scan pruning to limit computational complexity, and uses dual decomposition to solve the involved multi-frame assignment problem. The performance of the presented multi-target trackers, applied with an efficient fixed-lag smoothing method, are evaluated in a simulation study.

7.2 Paper B

Yuxuan Xia, Lennart Svensson, Ángel F. García-Fernández, Karl Granström, Jason L. Williams
Backward simulation for sets of trajectories
Published in 23rd International Conference on Information Fusion, Jul. 2020.

This paper presents a solution for recovering full trajectory information, via the calculation of the posterior of the set of trajectories, from a sequence of multitarget (unlabelled) filtering densities and the multitarget dynamic model. Importantly, the proposed solution opens an avenue of trajectory estimation possibilities for multitarget filters that do not explicitly estimate trajectories. In this paper, we first derive a general multitrajectory forward-backward smoothing equation based on sets of trajectories and the random finite set framework. Then we show how to sample sets of trajectories using backward simulation when the multitarget filtering densities are multi-Bernoulli processes. The proposed approach is demonstrated in a simulation study.

7.3 Paper C

Yuxuan Xia, Karl Granström, Lennart Svensson, Ángel F. García-Fernández, Jason L. Williams
Extended target Poisson multi-Bernoulli mixture trackers based on sets of trajectories

Published in 22nd International Conference on Information Fusion, Jul. 2019.

The Poisson multi-Bernoulli mixture (PMBM) is a multi-target distribution for which the prediction and update are closed. By applying the random finite set (RFS) framework to multi-target tracking with sets of trajectories as the variable of interest, the PMBM trackers can efficiently estimate the set of target trajectories. This paper derives two trajectory RFS filters for extended target tracking, called extended target PMBM trackers. Compared to the extended target PMBM filter based on sets on targets, explicit track continuity between time steps is provided in the extended target PMBM trackers.

7.4 Paper D

Yuxuan Xia, Pu Wang, Karl Berntorp, Lennart Svensson, Karl Granström, Hassan Mansour, Petros Boufounos, Philip V. Orlik
Learning based extended object tracking using hierarchical truncation measurement model with automotive radar
Submitted to IEEE Journal of Selected Topics in Signal Processing, 2020. .

This paper presents a data-driven measurement model for extended object tracking (EOT) with automotive radar. Specifically, the spatial distribution of automotive radar measurements is modeled as a hierarchical truncated Gaussian (HTG) with structural geometry parameters that can be learned from the training data. The HTG measurement model provides an adequate resemblance to the spatial distribution of real-world automotive radar measurements. Moreover, large-scale radar datasets can be leveraged to learn the geometry-related model parameters and offload the computationally demanding model parameter estimation from the state update step. The learned HTG measurement model is further incorporated into a random matrix based EOT approach with two (multi-sensor) measurement updates: one is based on a factorized Gaussian inverse-Wishart density representation and the other is based on a Rao-Blackwellized particle density representation. The effectiveness of the proposed approaches is verified on both synthetic data and real-world nuScenes dataset over 300 trajectories.

CHAPTER 8

Concluding remarks and future work

This thesis studies Bayesian object tracking problem for both point and extended objects with focus on MOT based on sets of trajectories. The concluding remarks and possible future work directions of the included papers are given as follows:

- **Paper A: "Multi-scan implementations of the trajectory Poisson multi-Bernoulli mixture filter"**
  This paper shows that multi-scan data association algorithms used in classical track-oriented MHT can be utilized in trajectory filters based on multi-object conjugate priors, resulting in the multi-scan implementations of the trajectory filters. An interesting future work is to benchmark the multi-scan trajectory filters against efficient track-oriented MHT algorithms in the literature.

- **Paper B: "Backward simulation for sets of trajectories"**
  This papers presented a general backward-forward smoothing equation for sets of trajectories and proposed a tractable implementation of a multi-trajectory smoother using backward simulation and ranked assignments. Though the proposed algorithm considers a batch solution, there

is still room for improvement on the computational efficiency of current implementation. The proof that the multi-object conjugacy also holds in the backward smoothing recursion should be done as well. Lastly, it would be interesting to consider a one-time-step lagged implementation of the multi-trajectory smoother, such that trajectories can be built upon the computation of multi-object filtering densities.

- **Paper C: "Extended target Poisson multi-Bernoulli mixture trackers based on sets of trajectories"**
  This paper presented an extended object PMBM tracker based on sets of trajectories that can directly produce trajectory estimates. Interesting future work directions include the developing of a smoothing-while-filtering GGIW implementation and a multi-scan extended object PMBM tracker that considers the multi-scan data association problem.

- **Paper D: "Learning-based extended object tracking using hierarchical truncation measurement model with automotive radar"**
  This paper presented a new measurement model for EOT with automotive radar by modeling the measurement spatial density as a HTG, which can be learned from real-world automotive radar data. The learned HTG measurement model has been further incorporated into a random matrix based EOT approach with two measurement updates based on two different density representations. To apply the proposed methods in more practical applications, follow-up directions include the integration of range rate measurements and the extension to multiple EOT.

References

[1] Y. Bar-Shalom, P. K. Willett, and X. Tian, *Tracking and data fusion*. YBS publishing Storrs, CT, USA: 2011, vol. 11.

[2] S. Challa, M. R. Morelande, D. Mušicki, and R. J. Evans, *Fundamentals of object tracking*. Cambridge University Press, 2011.

[3] S. Särkkä, *Bayesian filtering and smoothing*. Cambridge University Press, 2013, vol. 3.

[4] K. Granström, M. Baum, and S. Reuter, "Extended object tracking: Introduction, overview, and applications", *Journal of Advances in Information Fusion*, vol. 12, no. 2, 2017.

[5] K. Granström, L. Svensson, S. Reuter, Y. Xia, and M. Fatemi, "Likelihood-based data association for extended object tracking using sampling methods", *IEEE Transactions on intelligent vehicles*, vol. 3, no. 1, pp. 30–45, 2017.

[6] Y. Xia, P. Wang, K. Berntorp, T. Koike-Akino, H. Mansour, M. Pajovic, P. Boufounos, and P. V. Orlik, "Extended object tracking using hierarchical truncation measurement model with automotive radar", in *ICASSP 2020-2020 IEEE International Conference on Acoustics, Speech and Signal Processing (ICASSP)*, IEEE, 2020, pp. 4900–4904.

[7] Y. Xia, P. Wang, K. Berntorp, H. Mansour, P. Boufounos, and P. V. Orlik, "Extended object tracking using hierarchical truncation model with partial-view measurements", in *2020 IEEE 11th Sensor Array and Multichannel Signal Processing Workshop (SAM)*, IEEE, 2020, pp. 1–5.

[8] Y. Xia, P. Wang, K. Berntorp, P. Boufounos, P. V. Orlik, K. Granström, and L. Svensson, "Extended object tracking with automotive radar using learned structural measurement model", in *2020 IEEE Radar Conference (RadarConf)*, IEEE, 2020, pp. 1–6.

[9] S. Sun, A. P. Petropulu, and H. V. Poor, "MIMO radar for advanced driver-assistance systems and autonomous driving: Advantages and challenges", *IEEE Signal Processing Magazine*, vol. 37, no. 4, pp. 98–117, 2020.

[10] L. D. Stone, R. L. Streit, T. L. Corwin, and K. L. Bell, *Bayesian multiple target tracking*. Artech House, 2013.

[11] Y. Bar-Shalom, F. Daum, and J. Huang, "The probabilistic data association filter", *IEEE Control Systems Magazine*, vol. 29, no. 6, pp. 82–100, 2009.

[12] S. S. Blackman, "Multiple hypothesis tracking for multiple target tracking", *IEEE Aerospace and Electronic Systems Magazine*, vol. 19, no. 1, pp. 5–18, 2004.

[13] I. R. Goodman, R. P. Mahler, and H. T. Nguyen, *Mathematics of data fusion*. Springer Science & Business Media, 2013, vol. 37.

[14] R. P. Mahler, *Statistical multisource-multitarget information fusion*. Artech House, Inc., 2007.

[15] ——, *Advances in statistical multisource-multitarget information fusion*. Artech House, 2014.

[16] B.-T. Vo and B.-N. Vo, "Labeled random finite sets and multi-object conjugate priors", *IEEE Transactions on Signal Processing*, vol. 61, no. 13, pp. 3460–3475, 2013.

[17] J. L. Williams, "Marginal multi-Bernoulli filters: RFS derivation of MHT, JIPDA, and association-based MeMBer", *IEEE Transactions on Aerospace and Electronic Systems*, vol. 51, no. 3, pp. 1664–1687, 2015.

[18] Á. F. García-Fernández, J. L. Williams, K. Granström, and L. Svensson, "Poisson multi-Bernoulli mixture filter: Direct derivation and implementation", *IEEE Transactions on Aerospace and Electronic Systems*, vol. 54, no. 4, pp. 1883–1901, 2018.

[19] K. Granström, M. Fatemi, and L. Svensson, "Poisson multi-Bernoulli mixture conjugate prior for multiple extended target filtering", *IEEE Transactions on Aerospace and Electronic Systems*, vol. 56, no. 1, pp. 208–225, 2019.

[20] Á. F. García-Fernández, Y. Xia, K. Granström, L. Svensson, and J. L. Williams, "Gaussian implementation of the multi-Bernoulli mixture filter", in *2019 22th International Conference on Information Fusion (FUSION)*, IEEE, 2019, pp. 1–8.

[21] B.-N. Vo, B.-T. Vo, and D. Phung, "Labeled random finite sets and the bayes multi-target tracking filter", *IEEE Transactions on Signal Processing*, vol. 62, no. 24, pp. 6554–6567, 2014.

[22] M. Beard, S. Reuter, K. Granström, B.-T. Vo, B.-N. Vo, and A. Scheel, "Multiple extended target tracking with labeled random finite sets", *IEEE Transactions on Signal Processing*, vol. 64, no. 7, pp. 1638–1653, 2015.

[23] R. P. Mahler, "Multitarget Bayes filtering via first-order multitarget moments", *IEEE Transactions on Aerospace and Electronic systems*, vol. 39, no. 4, pp. 1152–1178, 2003.

[24] R. Mahler, "PHD filters of higher order in target number", *IEEE Transactions on Aerospace and Electronic systems*, vol. 43, no. 4, pp. 1523–1543, 2007.

[25] E. Brekke and M. Chitre, "Relationship between finite set statistics and the multiple hypothesis tracker", *IEEE Transactions on Aerospace and Electronic Systems*, vol. 54, no. 4, pp. 1902–1917, 2018.

[26] Á. F. García-Fernández, J. Grajal, and M. R. Morelande, "Two-layer particle filter for multiple target detection and tracking", *IEEE Transactions on Aerospace and Electronic Systems*, vol. 49, no. 3, pp. 1569–1588, 2013.

[27] E. H. Aoki, P. K. Mandal, L. Svensson, Y. Boers, and A. Bagchi, "Labeling uncertainty in multitarget tracking", *IEEE Transactions on Aerospace and Electronic systems*, vol. 52, no. 3, pp. 1006–1020, 2016.

[28] Á. F. García-Fernández, L. Svensson, and M. R. Morelande, "Multiple target tracking based on sets of trajectories", *IEEE Transactions on Aerospace and Electronic Systems*, vol. 56, no. 3, pp. 1685–1707, 2020.

[29] Á. F. García-Fernández and L. Svensson, "Trajectory PHD and CPHD filters", *IEEE Transactions on Signal Processing*, vol. 67, no. 22, pp. 5702–5714, 2019.

[30] K. Granström, L. Svensson, Y. Xia, J. L. Williams, and Á. F. García-Fernández, "Poisson multi-Bernoulli mixture trackers: Continuity through random finite sets of trajectories", in *2018 21st International Conference on Information Fusion (FUSION)*, IEEE, 2018, pp. 1–5.

[31] Á. F. García-Fernández, L. Svensson, J. L. Williams, Y. Xia, and K. Granström, "Trajectory Poisson multi-Bernoulli filters", *IEEE Transactions on Signal Processing*, vol. 68, pp. 4933–4945, 2020.

[32] W. Koch and F. Govaers, "On accumulated state densities with applications to out-of-sequence measurement processing", *IEEE Transactions on Aerospace and Electronic Systems*, vol. 47, no. 4, pp. 2766–2778, 2011.

[33] F. Lindsten and T. B. Schön, "Backward simulation methods for monte carlo statistical inference", *Foundations and Trends® in Machine Learning*, vol. 6, no. 1, pp. 1–143, 2013.

[34] R. M. Eustice, H. Singh, and J. J. Leonard, "Exactly sparse delayed-state filters for view-based slam", *IEEE Transactions on Robotics*, vol. 22, no. 6, pp. 1100–1114, 2006.

[35] Á. F. García-Fernández, L. Svensson, M. R. Morelande, and S. Särkkä, "Posterior linearization filter: Principles and implementation using sigma points", *IEEE transactions on signal processing*, vol. 63, no. 20, pp. 5561–5573, 2015.

[36] E. A. Wan and R. Van Der Merwe, "The unscented Kalman filter for nonlinear estimation", in *Proceedings of the IEEE 2000 Adaptive Systems for Signal Processing, Communications, and Control Symposium (Cat. No. 00EX373)*, Ieee, 2000, pp. 153–158.

[37] I. Arasaratnam and S. Haykin, "Cubature Kalman filters", *IEEE Transactions on automatic control*, vol. 54, no. 6, pp. 1254–1269, 2009.

[38] H. E. Rauch, F. Tung, and C. T. Striebel, "Maximum likelihood estimates of linear dynamic systems", *AIAA journal*, vol. 3, no. 8, pp. 1445–1450, 1965.

[39] S. Yang, M. Baum, and K. Granström, "Metrics for performance evaluation of elliptic extended object tracking methods", in *2016 IEEE International Conference on Multisensor Fusion and Integration for Intelligent Systems (MFI)*, IEEE, 2016, pp. 523–528.

[40] C. R. Givens, R. M. Shortt, *et al.*, "A class of Wasserstein metrics for probability distributions.", *The Michigan Mathematical Journal*, vol. 31, no. 2, pp. 231–240, 1984.

[41] D. Schuhmacher and A. Xia, "A new metric between distributions of point processes", *Advances in applied probability*, vol. 40, no. 3, pp. 651–672, 2008.

[42] D. Schuhmacher, B.-T. Vo, and B.-N. Vo, "A consistent metric for performance evaluation of multi-object filters", *IEEE transactions on signal processing*, vol. 56, no. 8, pp. 3447–3457, 2008.

[43] A. S. Rahmathullah, Á. F. García-Fernández, and L. Svensson, "Generalized optimal sub-pattern assignment metric", in *2017 20th International Conference on Information Fusion (Fusion)*, IEEE, 2017, pp. 1–8.

[44] Á. F. García-Femández and L. Svensson, "Spooky effect in optimal OSPA estimation and how GOSPA solves it", in *2019 22th International Conference on Information Fusion (FUSION)*, IEEE, 2019, pp. 1–8.

[45] X. R. Li and V. P. Jilkov, "Survey of maneuvering target tracking. Part I. Dynamic models", *IEEE Transactions on Aerospace and Electronic Systems*, vol. 39, no. 4, pp. 1333–1364, 2003.

[46] M. Feldmann, D. Franken, and W. Koch, "Tracking of extended objects and group targets using random matrices", *IEEE Transactions on Signal Processing*, vol. 59, no. 4, pp. 1409–1420, 2010.

[47] U. Orguner, "A variational measurement update for extended target tracking with random matrices", *IEEE Transactions on Signal Processing*, vol. 60, no. 7, pp. 3827–3834, 2012.

[48] K. Granström and U. Orguner, "New prediction for extended targets with random matrices", *IEEE Transactions on Aerospace and Electronic Systems*, vol. 50, no. 2, pp. 1577–1589, 2014.

[49] J. L. Williams, "Marginal multi-Bernoulli filters: RFS derivation of MHT, JIPDA, and association-based member", *IEEE Transactions on Aerospace and Electronic Systems*, vol. 51, no. 3, pp. 1664–1687, 2015.

[50] ——, "Hybrid Poisson and multi-Bernoulli filters", in *2012 15th International Conference on Information Fusion*, IEEE, 2012, pp. 1103–1110.

[51] Y. Xia, K. Granstrcom, L. Svensson, and Á. F. García-Fernández, "Performance evaluation of multi-Bernoulli conjugate priors for multi-target filtering", in *2017 20th International Conference on Information Fusion (Fusion)*, IEEE, 2017, pp. 1–8.

[52] Y. Xia, K. Granström, L. Svensson, and Á. F. García-Fernández, "An implementation of the Poisson multi-Bernoulli mixture trajectory filter via dual decomposition", in *Proceedings of the 21st International Conference on Information Fusion (FUSION)*, 2018.

[53] J. L. Williams, "An efficient, variational approximation of the best fitting multi-Bernoulli filter", *IEEE Transactions on Signal Processing*, vol. 63, no. 1, pp. 258–273, 2014.

[54] Y. Xia, K. Granström, L. Svensson, and M. Fatemi, "Extended target poisson multi-bernoulli filter", *arXiv preprint arXiv:1801.01353*, 2018.

[55] Á. F. García-Fernández, A. S. Rahmathullah, and L. Svensson, "A metric on the space of finite sets of trajectories for evaluation of multi-target tracking algorithms", *IEEE Transactions on Signal Processing*, vol. 68, pp. 3917–3928, 2020.

[56] K. Granström, L. Svensson, Y. Xia, Á. F. García-Fernández, and J. L. Williams, "Spatiotemporal constraints for sets of trajectories with applications to PMBM densities", in *2020 23rd International Conference on Information Fusion (FUSION)*, IEEE, 2020, pp. 1–8.

[57] K. Granström, L. Svensson, Y. Xia, J. Williams, and Á. F. García-Fernández, "Poisson multi-Bernoulli mixtures for sets of trajectories", *arXiv preprint arXiv:1912.08718*, 2019.